ELSEVIER

Channel response to tectonic forcing: field analysis of stream morphology and hydrology in the Mendocino triple junction region, northern California

Noah P. Snyder[a,*], Kelin X. Whipple[a], Gregory E. Tucker[b], Dorothy J. Merritts[c]

[a] Department of Earth, Atmospheric and Planetary Sciences, Massachusetts Institute of Technology, Cambridge, MA 02139-4307, USA
[b] School of Geography and the Environment, University of Oxford, Oxford OX1 3TB, England, UK
[c] Geosciences Department, Franklin and Marshall College, Lancaster, PA 17604-3003, USA

Abstract

An empirical calibration of the shear stress model for bedrock incision is presented, using field and hydrologic data from a series of small, coastal drainage basins near the Mendocino triple junction in northern California. Previous work comparing basins from the high uplift zone (HUZ, uplift rates around 4 mm/year) to ones in the low uplift zone (LUZ, ~ 0.5 mm/year) indicates that the HUZ channels are about twice as steep for a given drainage area. This observation suggests that incision processes are more effective in the HUZ. It motivates a detailed field study of channel morphology in the differing tectonic settings to test whether various factors that are hypothesized to influence incision rates (discharge, channel width, lithology, sediment load) change in response to uplift or otherwise differ between the HUZ and LUZ. Analysis of regional stream gaging data for mean annual discharge and individual floods yields a linear relationship between discharge and drainage area. Increased orographic precipitation in the HUZ accounts for about a twofold increase in discharge in this area, corresponding to an assumed increase in the erosional efficiency of the streams. Field measurements of channel width indicate a power-law relationship between width and drainage area with an exponent of ~ 0.4 and no significant change in width between the uplift rate zones, although interpretation is hampered by a difference in land use between the zones. The HUZ channel width dataset reveals a scaling break interpreted to be the transition between colluvial- and fluvial-dominated incision processes. Assessments of lithologic resistance using a Schmidt hammer and joint surveys show that the rocks of the study area should be fairly similar in their susceptibility to erosion. The HUZ channels generally have more exposed bedrock than those in the LUZ, which is consistent with protection by sediment cover inhibiting incision in the LUZ. However, this difference is likely the result of a recent pulse of sediment due to land use in the LUZ. Therefore, the role of sediment flux in setting incision rates cannot be constrained with any certainty. To summarize, of the four response mechanisms analyzed, the only factor that demonstrably varies between uplift rate zones is discharge, although this change is likely insufficient to explain the relationship between channel slope and uplift rate. The calibrated model allows us to make a prediction of channel concavity that is consistent with a previous estimate from slope–drainage area data. We show that the inclusion of nonzero values of critical shear stress in the model has important implications for the theoretical relationship between steady-state slope and uplift rate and might provide an explanation for

* Corresponding author. Now at: USGS Pacific Science Center, 1156 High Street, Santa Cruz, CA 95064, USA.
E-mail address: nsnyder@usgs.gov (N.P. Snyder).

the observations. This analysis underscores the importance of further work to constrain quantitatively threshold shear stress for bedrock incision.

1. Introduction

The response of river systems to tectonic, climatic, and land use perturbations is an area of active research in geomorphology (e.g., Merritts and Vincent, 1989; Tucker and Slingerland, 1997; Harbor, 1998; Tinkler and Wohl, 1998; Lavé and Avouac, 2000; Schumm et al., 2000; Kirby and Whipple, 2001). These efforts are motivated by the desire to develop a quantitative theory of the processes and styles of channel response, so that present-day stream morphology can be used to understand past disturbances. Bedrock rivers are particularly important to the goal of understanding tectonic–climatic–topographic interactions because incision into bedrock and transport of sediment controls the rates that (i) base-level signals (generated by tectonic, eustatic or climatic forcings) are transmitted through the landscape; and (ii) sediment is delivered from highlands to basins (Whipple and Tucker, 1999). To use bedrock rivers to gain insight into tectonic or climatic conditions, we must first understand how known changes in these forcings affect the channel morphology. Here we present field data from a site where the tectonic and climatic conditions are well known.

In a previous study of streams in the vicinity of the Mendocino triple junction region of northern California (Snyder et al., 2000), we used data from digital elevation models (DEMs) to compare stream longitudinal profiles from basins undergoing varying rock uplift rates, in terms of the shear stress model for bedrock incision. We found that the topography of the area was not easily explained by the simplest form of the model. Specifically, the streams showed an approximately twofold increase in slope (at a given drainage area) in response to an eightfold increase in rock uplift rate. This is considerably less steep than expected from the simplest form of the model, which assumes that (i) climate and lithology are the same throughout the field area, (ii) channels respond to changes in rock uplift rate through adjustments in channel gradient only, and (iii) the critical shear stress to initiate incision is negligible. This paper investigates the first two assumptions in detail using field data. Providing quantitative constraints on critical shear stress is beyond the scope of this work, but we do discuss the modeling implications of nonzero values of this parameter.

The observation that the channels do not exhibit a greater contrast in gradient can be interpreted to mean that, as rates of tectonic uplift increase, incision processes act more effectively. This paper tests hypotheses that this incision rate change might be the result of the response of four basic factors that control erosion rates: (i) increases in stream discharge because of orographic precipitation in the HUZ; (ii) narrowing of channel width in the HUZ; (iii) different lithologic resistance throughout the study area (weaker rocks in the HUZ); and (iv) changes in sediment flux (greater in the HUZ) or bed cover (greater in the LUZ). Below, we outline briefly how these adjustments might influence response to tectonic and climatic perturbations, and introduce means for field testing of these hypotheses.

Bedrock channel incision is driven by flood events (e.g., Baker and Kale, 1998). Mountainous topography can enhance the magnitude of large discharge events by increasing precipitation through orographic lifting of moist storm air masses (e.g., Barros and Lettenmaier, 1993). Therefore, mountain building by accelerated rock uplift rates can enhance incision processes. Through analysis of stream discharge records in varying settings, we can begin to quantify this tectonic–climatic–erosion feedback loop.

Rivers have been shown to respond to perturbations through adjustments in channel width (e.g., Harbor, 1998; Lavé and Avouac, 2000; Hancock and Anderson, 2002). Entrenchment within wide valley bottoms increases flow depth, therefore increasing basal shear stress, which drives incision. Previously,

we speculated that channels undergoing high uplift rates might be systematically narrower (Snyder et al., 2000). Here, we test this hypothesis by measuring channel widths throughout the field area. We also evaluate whether width–discharge–area scaling relations that are well known in alluvial rivers (Leopold and Maddock, 1953) hold for bedrock rivers (Montgomery and Gran, 2001), as is often assumed in landscape evolution models. In addition, these scaling relations yield insight into the study of downstream process transitions.

Any regional comparison of bedrock channel morphology must carefully evaluate lithologic resistance (e.g., Tinkler and Wohl, 1998). Harder, less fractured rocks will erode slowly, and weaker, more fractured rocks will erode more rapidly. Differing tectonic regimes might lead to different rock types, simply by juxtaposing distinct lithologic packages. In addition, topographic stresses set up by increased relief might drive fracturing of rocks in valley bottoms, as hypothesized by Miller and Dunne (1996). Quantification of lithologic resistance is difficult (Selby, 1993), and here we primarily attempt to discern whether important variations in rock strength exist in the field area.

If incision is driven by particle impacts with the bed, then sediment flux may influence bedrock incision rates and channel gradients (Sklar and Dietrich, 1998; Whipple and Tucker, 2002). At low sediment flux, the stream might have insufficient tools to incise the bed, whereas at higher sediment flux rates, incision might be optimized. However, if the sediment flux rate exceeds the transport capacity of the stream, then the bed might be protected—i.e., armored from incision by stored alluvium. These effects are difficult to quantify with field data, and perhaps the most promising avenues of research are through laboratory experiments (Sklar and Dietrich, 1999). Here, we make observations of channel bed morphology to gain some qualitative insight as to whether or not sediment flux plays an important role in setting incision rates throughout the field area.

The purpose of this paper is to provide a field-based empirical calibration of the shear-stress bedrock-incision model, with emphasis placed on testing hypothesized response mechanisms of streams to tectonics. We begin with a review of the model, with specific reference to which model parameters can be estimated from field data, and which are unknown (Section 2). Section 3 is a brief description of the important aspects of the tectonics and fluvial geomorphology of the field area. The empirical calibration is presented in Section 4, with four sections on stream discharge, channel width, lithologic resistance, and channel bed morphology. Each of these sections is divided into subsections on background, methods, results, and interpretations. In Section 5, the results of the calibration are discussed in terms of process transitions in the landscape, our previous work on longitudinal profiles and channel concavity (Snyder et al., 2000), and the role of threshold shear stresses in the model. Finally, we assess overall response of the channels to variable tectonic forcing, and suggest a few avenues for further investigations.

2. Theoretical background

Many workers have postulated that detachment-limited fluvial bedrock incision rate (E) is a power-law function of excess shear stress (e.g., Howard and Kerby, 1983; Howard, 1994; Parker and Izumi, 2000):

$$E = k_e(\tau_b - \tau_c)^a \tag{1}$$

where τ_b is shear stress at the channel bed, τ_c is a threshold (or critical) shear stress for detachment of bedrock blocks, k_e is a dimensional coefficient, and a is an exponent, assumed to be positive and constant. In this study, k_e, a, and τ_c are unknown parameters.

The value of a depends on the incision process. Theoretical considerations suggest that the shear stress exponent (a) should be around 3/2 for plucking of intact bedrock blocks, 5/2 for suspended-load (sand) abrasion, and possibly higher for cavitation (Whipple et al., 2000a). For this study, we assume incision processes (and therefore a) are constant throughout the studied channels.

The shear stress coefficient (k_e) depends on several factors:

$$k_e = k_e \text{ (erosion process, lithologic resistance,}$$

$$\text{sediment flux, intermittency factor)}. \tag{2}$$

Just as the exponent (a) varies with erosion process, so must the coefficient (k_e). Lithologic resistance will, of course, directly influence the rate that rivers can

incise, with more resistant rocks (harder, less jointed) corresponding to slower (low k_e) rates. Sediment flux and associated sediment carrying capacity of a river can be important controls on bedrock incision rate, as discussed by Sklar and Dietrich (1998, 2001). The intermittency factor is necessary in this approach because incision is assumed to happen during representative events which occur only during some small fraction of time (Paola et al., 1992; Tucker and Slingerland, 1997). Here we evaluate carefully how the factors that make up k_e can be expected to vary throughout a field area and in response to changes in tectonic regime.

Threshold shear stress (τ_c) is the minimum bed shear stress (τ_b) required to initiate detachment of bedrock blocks. It is often assumed that large flood events are responsible for most bedrock erosion and that τ_b is much greater than τ_c during such events, so τ_c is negligible in modeling efforts. We do not make this assumption in our analysis because, as we show below, the inclusion of a nonzero critical shear stress importantly influences the relationship between steady-state channel slope (S_e) and rock uplift rate (U). Like k_e, τ_c is expected to be a function of erosion process and lithologic resistance, as well as size of bed sediment.

We now place Eq. (1) in terms of more easily measured quantities, specifically drainage area (A) and local channel slope (S). We follow the basic approach of Howard and Kerby (1983). The purpose of reviewing this derivation is to highlight the components of the model that can be measured from field data. The assumptions of steady and uniform flow and conservation of momentum and water mass, combined with the Manning equation, yield the following relation for shear stress (τ_b):

$$\tau_b = \rho g N^\alpha \left(\frac{Q}{w}\right)^\alpha S^\beta \tag{3}$$

where ρ is the density of water; g is the acceleration due to gravity; Q is stream discharge; w is channel width; S is local channel gradient; and α and β are positive, constant exponents. In the roughness approach used here, $\alpha = 3/5$, $\beta = 7/10$, and N is the Manning coefficient (also used by Tucker and Bras, 2000). An alternative formulation using a dimensionless Darcy–Weisbach friction factor gives $\alpha = \beta = 2/3$

(Tucker and Slingerland, 1997; Whipple and Tucker, 1999; Snyder et al., 2000). We use the Manning equation formulation because it includes a dependence of flow discharge on flow depth that is likely to be appropriate for the rugged channels of the field area. This possibility is developed further in the discussion.

Next we put discharge (Q) and width (w) in terms of drainage area (A) via power-law relationships for basin hydrology,

$$Q = k_q A^c \tag{4}$$

and hydraulic geometry:

$$w = k_w Q^b = k_w k_q^b A^{bc} = k_w' A^{b'} \tag{5}$$

where k_w and k_q are dimensional coefficients, b and c are exponents, and $k_w' = k_w k_q^b$ and $b' = bc$. In this approach, the coefficient k_q corresponds to a dominant discharge event, responsible for most of the channel incision. The intermittency factor in Eq. (2) is time fraction of this discharge event. We present empirical data to constrain k_q, k_w', c, and b' using power-law regressions in the next section.

Combining Eqs. (1) and (3)–(5), we obtain the following relation for bed shear stress:

$$\tau_b = k_t A^{\alpha(c-b')} S^\beta \tag{6}$$

where $k_t = \rho g N^\alpha (k_q/k_w')^\alpha$, by definition. This approach implicitly assumes that the width exponent (b) is the same for downstream and at-a-station variations in channel width. If Q is a specific discharge event, this assumption is unimportant; but for general Q, both estimates of b are needed. Eq. (6) can be substituted into Eq. (1) to obtain the relation for channel incision as a function of drainage area (A), slope (S), and critical shear stress (τ_c):

$$E = k_e (k_t A^{\alpha(c-b')} S^\beta - \tau_c)^a \tag{7}$$

The relationship in Eq. (7), the shear stress model for bedrock incision by rivers, includes a nonzero critical shear stress term. Setting $\tau_c = 0$, we obtain the familiar version of this equation:

$$E = K A^m S^n \tag{8}$$

where the coefficient of incision K equals $k_e k_t^a$; the area exponent m equals $\alpha a(c - b')$; and the slope exponent n equals βa.

In the case of steady-state incision where rock uplift (U) is perfectly balanced by channel incision (E), we can solve Eq. (7) for steady-state slope (S_e):

$$S_e = \left[\left(\frac{U}{K} \right)^{1/a} + \left(\frac{\tau_c}{k_t} \right) \right]^{1/\beta} A^{-\frac{\alpha}{\beta}(c - b')} \qquad (9)$$

For $\tau_c = 0$, Eq. (9) reduces to the more familiar form:

$$S_e = \left(\frac{U}{K} \right)^{1/n} A^{-m/n} \qquad (10)$$

These equations predict a power-law relationship between slope (S) and area (A) that commonly is observed in rivers (e.g., Hack, 1973; Snyder et al., 2000). In the case of study-state channels, with spatially constant uplift rate (U) and other parameters (see discussion of steady-state channels in Snyder, 2000 #158), stream profile concavity index is given by the exponent on area ($(\alpha/\beta)(c - b') = m/n$), and channel steepness index is given by the coefficient ($[(U/K)^{1/a} + (\tau_c/k_t)]^{1/\beta}$ or $(U/K)^{1/n}$). Importantly, these relations predict that because channel concavity does not depend on a, it should be independent of incision process (Whipple and Tucker, 1999). Because the values of α and β are known, we can measure c and b' with power-law regressions of field data to get an empirical estimate of the channel concavity index. Later in this paper, we compare this calibrated concavity index to empirically derived values from longitudinal profiles (Snyder et al., 2000).

3. Field area and previous work

The field area comprises a series of small drainage basins along the northern California coast from Cape Mendocino south to Westport (Fig. 1). The region has a maritime, humid climate with wet winters and dry summers. These streams first were analyzed by Merritts and Vincent (1989) and subsequently by Snyder et al. (2000). The reader is referred to these sources for a full description of the area. Rock uplift rates vary in the field area from

$\sim$ 0.5 mm/year in the south to 4 mm/year in the King Range (Fig. 2). These rates were obtained from studies of a flight of Quaternary marine terraces exposed in the region (Merritts and Bull, 1989; Merritts and Vincent, 1989; Merritts, 1996). Following the terminology of Snyder et al. (2000), we divided the field area into four uplift rate zones (Fig. 2). In this study, we present field data from four streams in the high uplift zone (HUZ: Oat, Kinsey, Shipman, and Gitchell), two streams in the low uplift zone (LUZ: Hardy and Juan), and one stream in the zone of intermediate uplift rate that lies between the HUZ and the LUZ (Horse Mountain; Fig. 1). These basins were chosen because their profiles are representative of the uplift rate zones (Snyder et al., 2000) and they are relatively easy to access. Rock uplift rates in the HUZ accelerated around 100 ka from 0.5–1 mm/year to the present rate (Merritts and Bull, 1989).

The basins are small (drainage area 4–19 km^2), steep (up to 1200 m of relief), and forested. Near drainage divides, the streams begin as colluvial channels. Downstream, in the fluvial part of the system, the channel morphology is a locally variable mix of bedrock, step-pool, forced step-pool, and boulder-cascade conditions (classifications of Montgomery and Buffington, 1997). The mouths of most of the basins studied (particularly Shipman, Hardy, and Juan Creeks) have cobble to pebble plane-bed reaches. The LUZ basins are covered by dense forests, dominated by coast redwoods (*Sequoia sempervirens*), with immature riparian forests on flood plains near the mouths. The HUZ basins have grassy ridgetops, and hillslopes covered by Douglas fir (*Pseudotsuga menziesii*).

In our previous study (Snyder et al., 2000), we analyzed stream longitudinal profile data derived from digital elevation models for a series of 21 streams in the study area. The analysis, based on the standard shear stress model ($\tau_c = 0$, Eqs. (8) and (10)), demonstrated that the observed relationship between channel slope and uplift rate could be explained only by either an unrealistically high value of the slope exponent ($n \approx 4$) or a significant increase in the coefficient of erosion (K) in the HUZ. This result implies that erosion processes are acting more efficiently in the HUZ—a conclusion that motivates further analysis of channel response mechanisms and feedbacks. We also
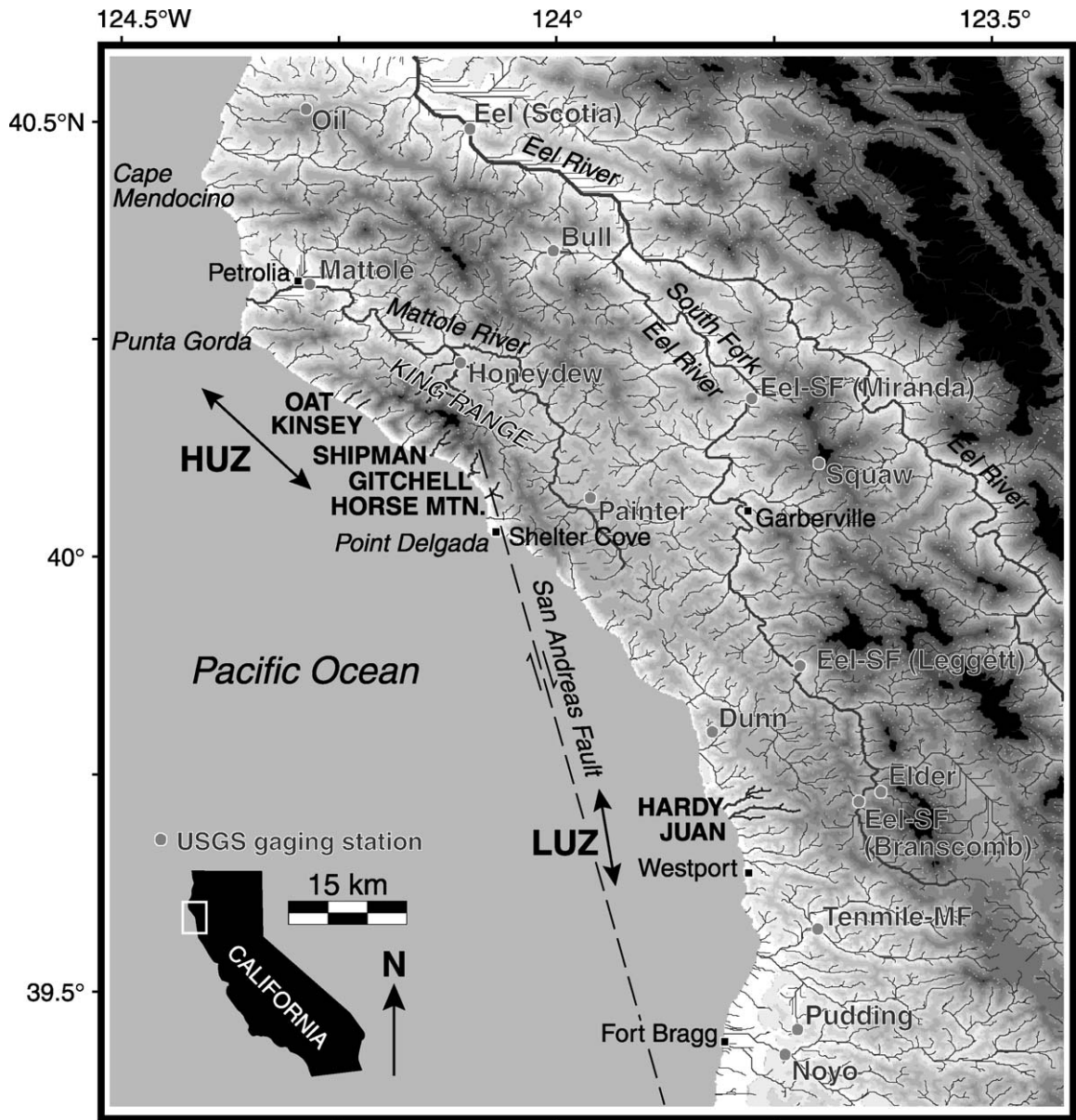
Fig. 1. Map of the Mendocino triple junction area, including the drainage network and elevation shading. Drainage network includes all streams with drainage area $(A) > 1$ km^2. Rivers and creeks mentioned in the text are shown with bold lines. The seven field-studied creeks are marked with capital letters at their mouths and are separated into high uplift zone (HUZ) and low uplift zone (LUZ) channels. Elevation shading ranges from white for 0–100 m to black for all areas >1000 m. USGS gaging stations used in this study are indicated by dots.

included an attempt to characterize, to first order, the role of precipitation differences between the LUZ and HUZ. We found that orographic enhancement of stream discharge could only partially explain the observed channel slope–uplift rate relationship. We also included some preliminary channel width data from the HUZ. Here, we expand significantly on these prior analyses by using a more complete suite of field
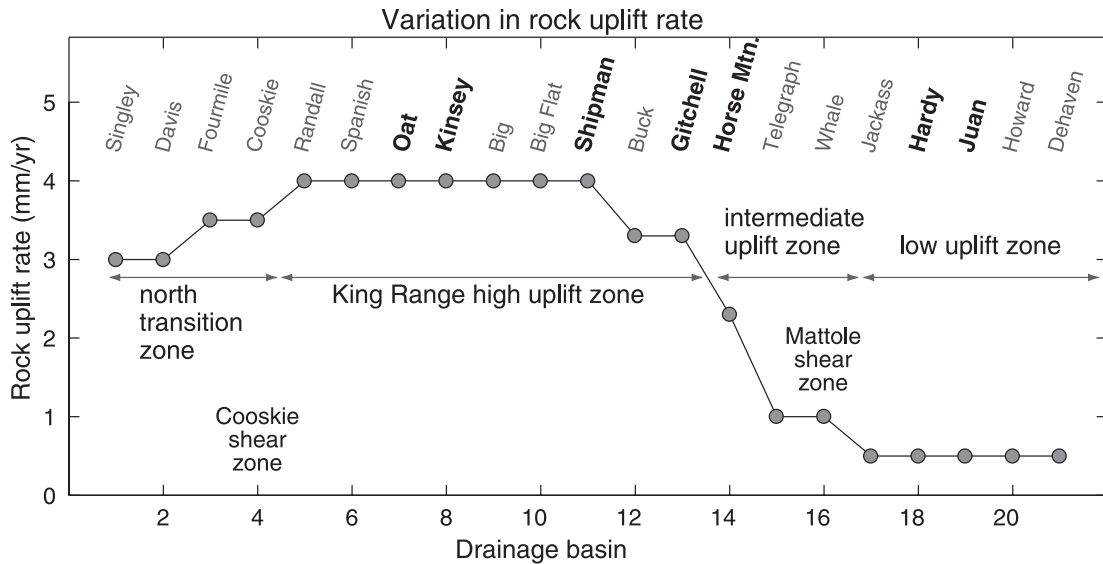
Fig. 2. Latest Pleistocene to Holocene rock uplift rates (U) for the 21 basins included in this and our previous study (Snyder et al., 2000), from north to south. The seven field-studied basins are in bold. Data are from Merritts and Bull (1989).

and hydrologic data, as well as a fuller version of the shear stress model.

4. Empirical calibration of the shear stress model

To gain a quantitative understanding of channel response to differing rock uplift rates in terms of the shear stress model, we evaluated four parameters of the study area: stream discharge, channel width, lithologic resistance, and stream bed morphology. Below, we present data and analysis pertinent to each of these four factors. Each analysis is divided into four subsections. In the background subsection, we look at: (i) previous empirical and/or theoretical work, both in general and in adjacent field areas; and (ii) how the parameters may be affected by differing rock uplift rates. The subsection on methods describes the data collection and analysis techniques. Each part closes with subsections on results and interpretations.

4.1. Discharge

4.1.1. Background

Many previous studies have shown that stream discharge increases with drainage area for streams in nonarid regions. Eq. (4) is a commonly assumed and observed empirical relationship between drainage area (A) and stream discharge (Q) (Leopold et al., 1964; Dunne and Leopold, 1978; Talling, 2000). Empirical values for the exponent c depend on the discharge measurement: from $c = 1$ for mean annual discharge, to $c \approx 0.7 - 0.9$ for bankfull discharge in alluvial channels (Dunne and Leopold, 1978). Values of c for individual flood events of greater magnitude than bankfull have received less attention in the literature, although because these are likely the important erosive events (Baker and Kale, 1998), we suspect that this discharge measurement may be most useful for our purposes.

In the simplest case of constant rainfall intensity over an entire basin with complete runoff (either through saturation or Horton overland flow), the value of the exponent c is unity, and the value of the coefficient (k_q) will simply be the rainfall intensity (Dunne and Leopold, 1978). However, particularly in larger basins and/or short rainfall events, storm contributions to stream discharge might not be equal throughout the entire basin, causing c to be < 1. This can happen for at least two reasons: (i) water storage and slow transport in the subsurface; or (ii) variations in rainfall intensity throughout a basin (Leopold et al., 1964). These effects are attenuated by long-term averaging, hence the linear

relationship observed for mean annual discharge (Dunne and Leopold, 1978).

Significant rainfall gradients exist in the Mendocino triple junction area because of orographic enhancement of precipitation by mountains. This is particularly true in the high uplift zone (HUZ), which is one of the wettest places in California (Rantz, 1968). Monitoring stations in Honeydew and Whitethorn, just inland from the crest of the King Range, receive 2.7 to 3.5 m/year of precipitation (National Climatic Data Center; Bureau of Land Management) compared with 0.98 m/year in Eureka and 1.01 m/year in Fort Bragg (Western Regional Climate Data Center) just to the north and south of the field area, respectively (Fig. 1). This contrast led us to make the simple assumption that the value of k_q may be as much as three times higher in the HUZ than the LUZ (Snyder et al., 2000). Here, we test this assumption through the use of stream gaging data. This analysis assumes that the relative differences seen in the current climate of the area are representative of the role of orography over the past ~ 100 ka.

4.1.2. Methods

To parameterize Eq. (4), we regressed discharge against drainage area. Because we suspected that c should be near unity, we calculated both a power-law and a linear least-squares best fit and associated 95% confidence intervals on the parameters (Hamilton, 1992). For the linear model, the intercept was forced at zero because Q must be zero with no upstream contributing area.

The U.S. Geological Survey (USGS) maintains numerous stream gaging stations throughout northern California. Unfortunately, none of the small coastal streams within the study area are monitored. Therefore, to find values of k_q and c, we needed to use data from elsewhere in the region as a proxy. We compiled data from 13 gaging stations that surround the study area (Fig. 1). These stations span a range of drainage area from 0.4 to 1840 km^2 (Table 1). The time series of measurements available from the USGS differ for each of the gaging stations (Table 1). Because of the northwest, coast-parallel flow direction of the South Fork of the Eel River, it is concentric to the entire field area; and we use its course as an outer border of the stations involved in the analysis (Fig. 1). Therefore, these stations do not include drainage area that is too far away from the study area, ensuring that the climate and hydrology is approximately constant throughout the region. We intentionally did not use data from the main trunk of the Eel River in the analysis because this river

Table 1
Discharge (Q) data for selected events (see Fig. 1 for gaging-station locations)[a]

Station	Drainage area, A ($\times 10^6$ m^2)	Length of record (years)	12/20–22/64 Q (m^3 s^{-1})	Event rank	1/15/1974 Q (m^3 s^{-1})	Event rank	3/17/1975 Q (m^3 s^{-1})	Event rank	1973–1976 mean annual Q (m^3 s^{-1})
Honeydew	51.1	4	nd	nd	130.26	2	139.32	1	4.23
Oil	0.45	12	0.71	1	nd	nd	nd	nd	nd
Squaw	0.89	10	2.46	2	nd	nd	nd	nd	nd
Painter	2.20	12	10.08	1	nd	nd	nd	nd	nd
Dunn	6.45	12	8.10	1	nd	nd	nd	nd	nd
Elder	22.3	32	103.64	1	56.07	4	25.66	9	0.83
Pudding	42.9	9	56.63	1	nd	nd	nd	nd	nd
Bull	96.4	38	184.63	2	165.10	5	93.16	19	3.76
Tenmile-MF	113	10	160.56	1	122.90	2	nd	nd	nd
Eel-SF-Bran	151	29	557.84	2	nd	nd	229.08	11	nd
Noyo	364	47	679.60	2	747.56	2	208.13	22	7.19
Mattole	841	50	2222.87	2	1758.50	3	1732.99	5	40.32
Eel-SF-Leggett	851	34	2228.54	1	1713.20	3	1019.41	8	28.52
Eel-SF-Miranda	1840	59	5635.05	1	3454.70	5	2650.46	9	62.71
Eel-Scotia	10,680	87	21,294.30	1	10,958.60	3	6541.20	26	254.92

[a] Rank indicates position of event in the series of mean-annual floods over the record of available data for each station. nd, no data available. Tenmile-MF, Middle Fork Tenmile River. Eel-SF, South Fork Eel River. Data for the Eel River at Scotia is included in this table only for comparison purposes because of its long length of record, it is not included in the regression analysis (Fig. 3; Table 2).

samples an area that extends far inland (Fig. 1; Table 1).

Because we are concerned with the relative difference in k_q between the HUZ and the LUZ (Snyder et al., 2000), we compared the discharge measured at Honeydew Creek in Honeydew, CA to the regression line for the other stations. The drainage area for Honeydew Creek is the east side of the King Range, so this station is likely to be the best representation of the HUZ drainages (Fig. 1). Unfortunately, only 4 years of data were available for Honeydew Creek (1973–1976; Table 1). Because most incision is likely to happen during storm events (Tinkler and Wohl, 1998), we compared the two largest floods gaged at Honeydew (January 15, 1974 and March 17, 1975) to data from the other stations during these events. In addition, we calculated mean annual discharge for the period of record on Honeydew Creek. Finally, to constrain the values of k_q and c for a major event, we compiled available data for the December 20–22, 1964 event, the largest flood on record for most of the stations in the region (Table 1; Wannanen et al., 1971).

4.1.3. Results

Fig. 3 shows the power-law and linear regressions of discharge against drainage area for three floods and the mean annual discharge in 1973–1976. All the datasets show linear trends in logarithmic space, and the power-law regressions indicate values of c that are indistinguishable from unity. The more complete discharge dataset from the December 1964 flood indicates that the scaling trend holds over four orders of magnitude in drainage area, including smaller basins on the order of those studied herein (0.1–20 km^2; Fig. 3A).

4.1.4. Interpretations

We find that for this field area discharge has a linear relationship with drainage area, and therefore the values of k_q for the linear model are most appropriate to use. The value of k_q from the regression lines corresponds to the magnitude of the associated flood, with the December 1964 event by far the largest.

For Honeydew Creek gage data, the discharge–area coordinate values lie above the regression line (Fig. 3B–D), consistent with the increase in precip-

itation observed at nearby rain gages. Table 2 shows values of k_q for Honeydew Creek, calculated using an assumed linear relationship between discharge and drainage area. With the best-fit values of k_q from the regression lines, Honeydew Creek transmits 1.3 to 2.3 times more discharge (relative to unit drainage area) than the rest of the area (Table 2). Taking the maximum cases from the confidence intervals on k_q, the range is 1.2 to 3.6. The threefold variation in k_q assumed by Snyder et al. (2000) is at the high end of these ranges. The flood of March 17, 1975 was the largest event of the short record for Honeydew Creek, and clearly a more significant event there than at other stations (ranking fifth at the adjacent Mattole River station and not more than eighth elsewhere; Table 1). However, the best-fit k_q for this event implies only a 1.9-times variation between Honeydew Creek and elsewhere, which is not quite as significant as might be expected (Table 2). The mean annual discharge data for Honeydew Creek shows the greatest deviation from the regression line of regional data, suggesting that Honeydew Creek has a significantly higher base flow than other streams in the region. This regression also has a closer match to the observed differences in annual precipitation.

Although we have no discharge data directly from the study-area channels, the proxy data from nearby streams suggest that we should expect an approximately twofold variation in the value of k_q between the HUZ and the LUZ. This interpretation is uncertain because we do not know whether the west side of the King Range is actually receiving more precipitation than the east side where Honeydew Creek is located. This situation might be expected, because the orographic effect is usually more pronounced on the seaward side of mountain ranges. However, three observations suggest that this may not be the case in this field area. First, the seaward side of the range is so narrow (<5 km) and steep that it might act as a barrier to precipitation, deflecting storms to the north and up the Mattole and Honeydew Valleys (Fig. 1). This is certainly the behavior exhibited by the ubiquitous northern California coastal fog in the area. Second, vegetation on the west side of the King Range is characteristic of a drier climate than that on the east side, although this might be a function of windier conditions and steeper slopes. Finally, the steep topographic gradient of the King
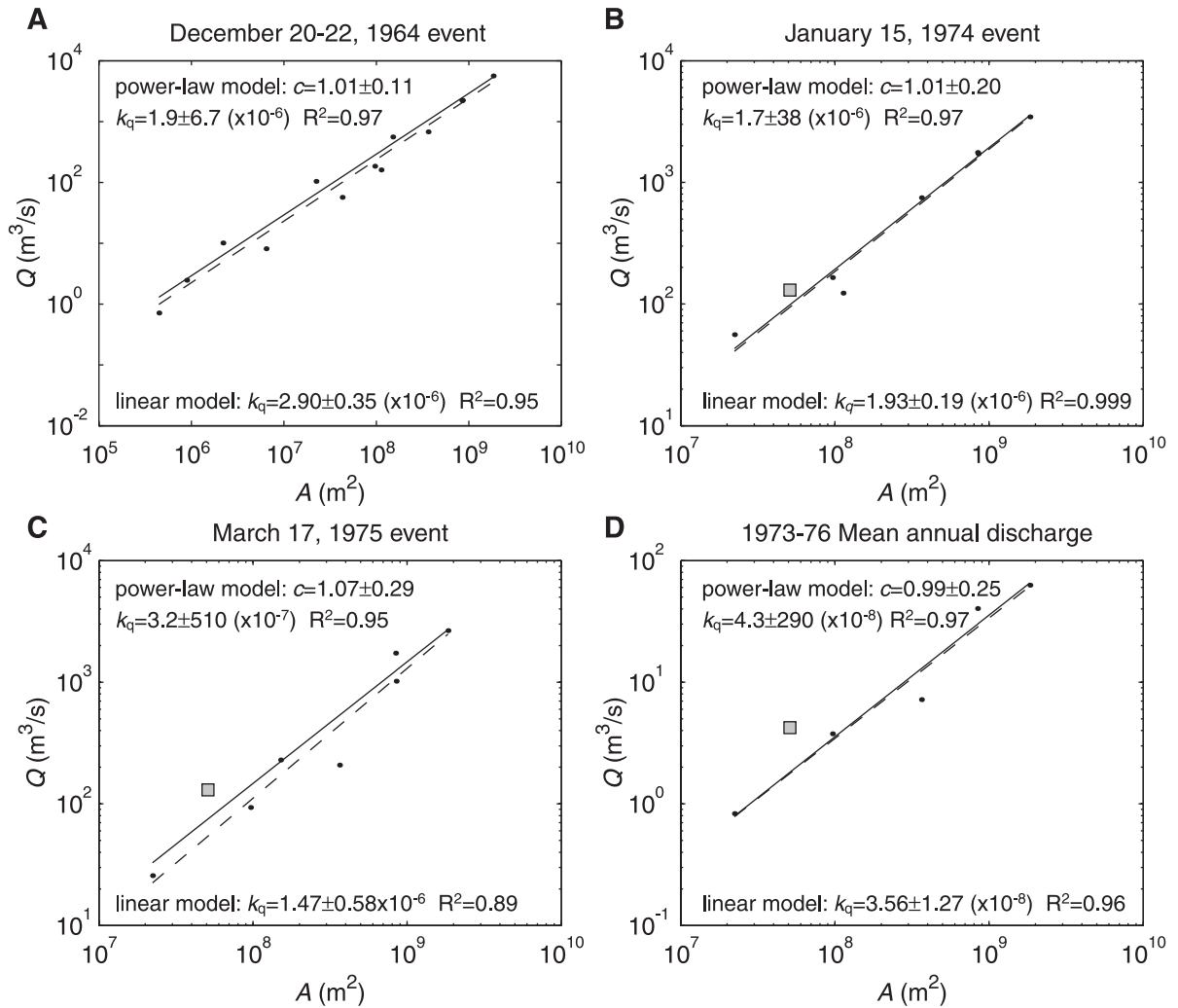
Fig. 3. Graphs of discharge vs. drainage area in logarithmic space. Solid circles are data points from USGS gaging stations. Gray box is the gaging station data for Honeydew Creek, which is not included in the regressions. Data is in Table 1. Dashed lines are least-squares, best-fit regression lines for a power-law model; solid lines are for a linear model. Regression data is in Table 2.

Range might enhance precipitation through lifting of air masses but, because of the small width of the seaward side, much of this precipitation might actually fall on the leeward side. For these reasons, the Honeydew Creek basin might actually receive more rainfall than the studied HUZ channels. Therefore, estimates of orographic enhancement of discharge presented in Table 2 are likely maxima when applied to the HUZ.

These uncertainties stated, we considered it reasonable to assume a twofold variation in flood-event k_q between the HUZ and LUZ, somewhat less than the up to threefold variation in annual precipitation. However, we are unable to place any constraints on the absolute magnitude of k_q, because to do so would assume a dominant discharge that is responsible for most channel incision. This value of k_q could correspond to a small-magnitude, high-recurrence flood (like the 1974 and 1975 events) or a very large, catastrophic event (perhaps greater than the 1964 event). This limitation is investigated further in the discussion section below.

Table 2
Discharge–drainage area coefficient (k_q) calculations[a]

Event	Number	c (power law) $\pm$ 95%	k_q (linear, $c=1$) (m s^{-1}) $\pm$ 95%	k_q(H) (m s^{-1})	k_q(H)/k_q	k_q(H)/$k_{q\ max}$	k_q(H)/$k_{q\ min}$
12/20–22/64	12	1.01 ± 0.11	2.90 ± 0.35 ($\times 10^{-6}$)	nd	nd	nd	nd
1/16/74	7	1.01 ± 0.20	1.93 ± 0.19 ($\times 10^{-6}$)	2.55×10^{-6}	1.32	1.46	1.20
2/17/75	7	1.07 ± 0.29	1.47 ± 0.58 ($\times 10^{-6}$)	2.73×10^{-6}	1.85	3.05	1.33
1973–1976 mean	6	0.99 ± 0.25	3.56 ± 1.27 ($\times 10^{-8}$)	8.28×10^{-8}	2.33	3.62	1.71

[a] k_q (H), best-fit value of k_q for Honeydew Creek. nd, no data available.

4.2. Channel width

4.2.1. Background

Hydraulic geometry in alluvial channels (relations among channel width, depth, and discharge) has received much research attention over the past 50 years (e.g., Leopold and Maddock, 1953; Richards, 1982). Eq. (5) describes the downstream trend in channel width with discharge (or via Eq. (4), area). The value of the exponent (b) has been shown to be ~ 0.5 in many studies of width and discharge in alluvial rivers (e.g., Leopold and Maddock, 1953). However, comparably little research has been done for bedrock-incision-dominated mountain channels like the ones in the study area, although a value of 0.5 is often assumed in models (e.g., Tucker and Bras, 2000). Recent interest in bedrock channel processes has yielded some studies of the Eq. (5) relationship for bedrock rivers (Pazzaglia et al., 1998; Snyder et al., 2000; Montgomery and Gran, 2001). In the most detailed study to date, Montgomery and Gran (2001) present width–drainage area data from a variety of ountain rivers in Washington, Oregon, and California indicating best-fit values of b from 0.30 to 0.53. The value of the width coefficient, k_w, should depend on a variety of factors including the location of the width measurement (high-flow channel, valley bottom, see below); the type of river (bedrock, plane bed, meandering, etc.); and the substrate (bedrock, fine or coarse alluvium).

Width adjustments are an important way in which fluvial systems might respond to perturbations (e.g., Harbor, 1998; Lavé and Avouac, 2000; Schumm et al., 2000; Hancock and Anderson, 2002). In our previous work, we speculated that bedrock channels are likely to narrow in response to increased gradients associated with higher uplift rates (Snyder et al., 2000). Like orographic precipitation, this is a feed-back mechanism that would make incision processes more effective in concert with higher uplift rates. This hypothesis predicts a lower value of k_w in the HUZ than in the LUZ and is easily testable with field data.

4.2.2. Methods

During the summers of 1998, 1999, and 2000, we conducted field surveys of seven study-area creeks (from north to south): Oat, Kinsey, Shipman, Gitchell, Horse Mountain, Hardy and Juan (Table 3). During these surveys, we collected several sets of data through measurements and observations: streamwise distance (using a hip chain) and local slope (using a hand inclinometer); channel width at stations spaced every 50 m in stream distance; rock strength and jointing (discussed in Section 4.3); stream bed morphology (discussed in Section 4.4); and terrace type (strath, fill) and height. At each station, three channel width measurements were made. (i) Low-flow width, defined by the water in the channel during summer baseflow conditions. (ii) High-flow width, defined as the zone of active scour between channel banks, generally seen as the area without vegetation. This width is analogous to the bankfull width of an alluvial river, and it is the measurement reported by Montgomery and Gran (2001). However, unlike Montgomery and Gran, we did not separate bedrock from alluvial channel reaches. (iii) Valley-bottom width from sidewall to sidewall, including strath and fill terraces to 3–4 m height above the stream bed. To further characterize local variability, a second set of high-flow width (and in Hardy Creek, valley width) measurements were made at each station during our later field seasons (including upper Oat, upper Kinsey, Gitchell, Horse Mountain, and Hardy Creeks). Most width measurements were made using a plastic tape measure, with an accuracy of 0.1 m. In some cases, valley width was found using a laser range-

Table 3
Channel width data

Creek	A (km^2)	U (mm/year)	Number	b'	k'_w	Width at 1 km^2 (m) (95% range)[a]	R^2	Regression survey range (km^2)[b]
High flow width								
(1) Oat	4.1	4	102	0.34 ± 0.07	0.045 ± 0.077	4.5 (4.2–4.9)	0.51	0.1–4.1
(2) Kinsey	3.9	4	67	0.56 ± 0.12	0.0026 ± 0.0074	5.8 (5.1–6.5)	0.62	0.1–0.4; 0.9–3.9
								0.3–0.4 (upper left trib)
(3) Shipman	8.7	4	49	0.46 ± 0.32	0.0094 ± 0.7215	5.6 (3.1–10)	0.15	3.3–8.7
(4) Gitchell	8.4	3.7	193	0.21 ± 0.04	0.354 ± 0.521	6.1 (5.8–6.5)	0.34	0.1–1.6
								2.4–8.6
HUZ (1–4)	4.1–8.7	3.7–4	411	0.35 ± 0.04	0.045 ± 0.065	5.4 (5.1–5.7)	0.49	0.1–8.7
(5) Horse Mtn.	6.9	~ 2	181	0.36 ± 0.05	0.031 ± 0.480	4.5 (4.2–4.8)	0.50	0.1–6.8
								1.8–3.5 (lower left trib)
(6) Hardy	13.0	0.5	311	0.22 ± 0.03	0.208 ± 0.296	4.0 (3.9–4.2)	0.36	0.1–10.5
								0.1–0.2 (North Fork)
								1.2–3.3 (North Fork)
(7) Juan	19.4	0.5	179	0.33 ± 0.03	0.040 ± 0.057	3.9 (3.6–4.2)	0.69	0.1–13.6; 14.4–19.1
								0.1–1.1 (upper left trib)
LUZ (6–7)	13.0–19.4	0.5	490	0.28 ± 0.02	0.090 ± 0.127	4.0 (3.8–4.2)	0.53	0.1–19.1
Valley width								
(1) Oat	4.1	4	93	0.41 ± 0.10	0.028 ± 0.067	7.7 (6.9–8.7)	0.42	0.1–4.1
(2) Kinsey	3.9	4	58	0.50 ± 0.14	0.0072 ± 0.0268	6.9 (6.0–7.9)	0.51	0.1–0.4; 0.9–3.9
								0.3–0.4 (upper left trib)
(3) Shipman	8.7	4	49	0.50 ± 0.47	0.0066 ± 4.8360	6.8 (2.9–16)	0.09	3.3–8.7
(4) Gitchell	8.4	3.7	100	0.32 ± 0.09	0.118 ± 0.246	9.7 (8.5–11)	0.37	0.1–1.6
								2.4–8.6
HUZ (1–4)	4.1–8.7	3.7–4	300	0.42 ± 0.05	0.023 ± 0.035	7.9 (7.4–8.5)	0.49	0.1–8.7
(5) Horse Mtn.	6.9	~ 2	96	0.42 ± 0.08	0.026 ± 0.050	8.8 (8.0–9.7)	0.56	0.1–6.8
								1.8–3.5 (lower left trib)
(6) Hardy	13.0	0.5	302	0.29 ± 0.04	0.181 ± 0.266	9.6 (9.0–10)	0.38	0.1–10.5
								0.1–0.2 (North Fork)
								1.2–3.3 (North Fork)
(7) Juan	19.4	0.5	170	0.46 ± 0.06	0.012 ± 0.020	7.2 (6.4–8.0)	0.60	0.1–13.6
								0.1–1.1 (upper left trib)
LUZ (6–7)	13.0–19.4	0.5	472	0.35 ± 0.03	0.072 ± 0.103	8.9 (8.4–9.4)	0.47	0.1–13.6

[a] Parenthetical range is the 95% confidence interval on the calculation of the mean width at 1 km^2 from the regression line (Fig. 4; Hamilton, 1992).

[b] Notes on regression ranges (all numbers are drainage areas). All data with $A < 0.1$ km^2 omitted from regressions. Data is from main trunk channel unless otherwise noted. Specific stream notes:

1. Oat Creek, entire stream surveyed.
2. Kinsey Creek, main trunk from 0.9 km^2 to mouth (3.9 km^2) and upper left tributary from 0.3 km^2 to junction with main channel (0.4 km^2) surveyed in 1998; main trunk from 0.1 to 0.4 km^2 surveyed in 1999 (stopped by waterfall).
3. Shipman Creek, main trunk from 3.3 km^2 to mouth (8.7 km^2) surveyed, stopped by waterfall.
4. Gitchell Creek, section between 1.6 and 2.4 km^2 could not be accessed due to waterfalls.
5. Horse Mountain Creek, entire stream surveyed; regressions also include some data from a large left tributary.
6. Hardy Creek, did not survey main trunk from 10.5 km^2 to mouth (13.0 km^2); regressions include some data from the upper (from the divide down) and lower sections (up from junction with main trunk) of the North Fork of Hardy Creek.
7. Juan Creek, did not survey main trunk from 13.6 km^2 to mouth (19.4 km^2), except a few high flow width measurements around the junction of Little Juan Creek from 14.4 to 19.1 km^2; regression also includes data from a left tributary near the divide.

finder (± 1 m) or visually estimated. Some sections of Kinsey, Shipman, and Gitchell Creeks could not be accessed, usually because of waterfalls (Table 3). The lower parts of Hardy and Juan Creeks were not accessed because of land ownership and time constraints, respectively (Table 3). To further augment

our data, we collected data from several tributary channels, selected because they appeared representative of the overall stream morphology and/or filled gaps in the span of drainage area surveyed (Table 3).

Because there are no gaging stations on the study-area streams, we plotted width against drainage area using Eq. (5) as a regression model. Drainage areas were calculated from DEMs and carefully registered to the field surveys. This process was checked by matching tributary junctions, which were recorded on field surveys and were easily recognized as step-function changes in the drainage area. The regression analysis included only data with $A > 10^5$ m^2, as this is the zone of fluvial process dominance in these channels identified by Snyder et al. (2000). We do not present data for the low-flow width because this is not geomorphically relevant and depends on the hydrologic conditions at the time of the measurement. The values of b' produced by the regressions were compared using the 95% confidence intervals on the regression parameter (Hamilton, 1992). Values of k'_w covary strongly with b', so we compared the widths predicted by the regressions at a reference drainage area of 10^6 m^2 (1 km^2) to test for systematic differences in channel width between the uplift rate zones. The ranges of predicted mean width values were compared using the 95% confidence hyperbolae on the regression (Table 3; Hamilton, 1992).

4.2.3. Results

Regressions of high-flow width against drainage area for individual streams yielded best-fit values of b' from 0.21 to 0.56, and valley width regressions ranged from 0.29 to 0.50 (Table 3). To increase the span of drainage areas included in the regressions and to characterize overall trends in the study area, we pooled data from the four HUZ streams surveyed (Oat, Kinsey, Shipman, and Gitchell Creeks) and the two LUZ streams (Hardy and Juan Creeks; Fig. 4; Table 3). These combined datasets yielded b' values of 0.35 ± 0.04 and 0.28 ± 0.02 for high-flow width of HUZ and LUZ streams, respectively. These ranges are significantly different within a 95% confidence interval. The combined datasets indicate valley width b' values of 0.42 ± 0.05 and 0.35 ± 0.03, respectively, which are not significantly different. The regression lines give best-fit high-flow widths of 5.4 and 4.0 m at the reference drainage area (1 km^2), respectively,

with ranges that do not overlap within 95% confidence intervals (Fig. 4; Table 3). Valley widths are 7.9 and 8.9 m, respectively, which do overlap (Fig. 4; Table 3).

4.2.4. Interpretations

The channel width measurements are quite variable, with nearly an order of magnitude of scatter at any drainage area (Fig. 4). Both the scatter and the range of b values are in good agreement with the data presented by Montgomery and Gran (2001). Combining the data from channels within uplift rate zones generally improves the regressions and, more importantly, allows us to analyze data over a larger span of drainage area in the HUZ (Table 3). For these reasons, we focus this discussion on the pooled-data regressions.

Comparison of b values for high-flow width data from the two uplift rate zones indicates that the regressions are significantly different, with a stronger relationship between width and area in the HUZ (Fig. 4). Surprisingly, the HUZ channels are significantly wider (at a given drainage area) than the LUZ channels, counter to the expected narrowing (Table 3; Snyder et al., 2000). Unfortunately, differences in recent land-use practices in the two zones complicate interpretation of these data. The more accessible topography and larger trees of the LUZ have made this area more attractive for logging. The four studied HUZ basins have never been logged significantly, whereas Juan and Hardy Creeks have had large-scale timber harvests for over a century. Past logging activity included the construction of an elevated railroad in the channel bottom of Hardy Creek and a road next to the channel in Juan Creek (Fig. 5). The channel morphology of Hardy and Juan Creeks reflects these land use practices, with ubiquitous fill terraces 1- to 2.5-m-high that are likely the result of increased sediment flux from harvested hillslopes and valley wall excavation for road construction. The terraces record recent entrenchment by the channel and are likely to be the reason the LUZ channels are narrower at present. Unfortunately, no low uplift channels in the field area share the land use history of the high uplift channels, and vice versa.

Horse Mountain Creek basin also was logged in the 1950s and 1960s and exhibits morphology similar to that of Hardy and Juan Creeks. Horse Mountain
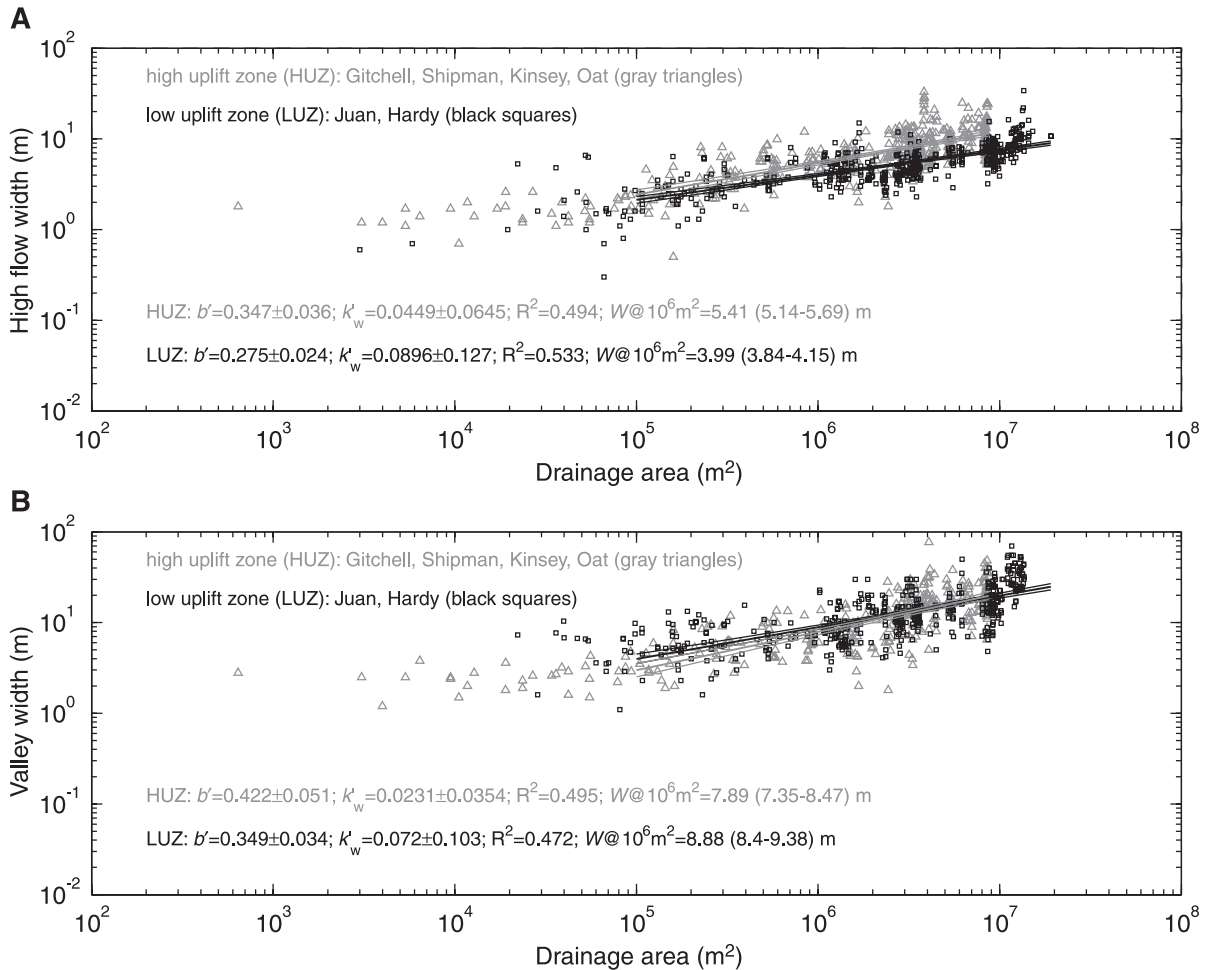
A

B

Fig. 4. Graphs of width vs. drainage area for (A) high-flow width and (B) valley width. High uplift zone data are gray triangles, low uplift zone data are black squares. Lines are least-squares best-fit power-law regressions (heavy lines), with associated 95% confidence hyperbolae (fine lines), for the two datasets, with $A > 10^5$ m^2 (Hamilton, 1992). See Table 3 for data for individual streams.

Creek has a high-flow width of 4.2–4.8 m at 1 km^2, overlapping with the range seen on the LUZ creeks (Table 3). For these reasons, we believe that the differences between high-flow widths throughout the field area should not be viewed as the result of differing response to uplift rates.

We next turn to the valley width data, which are less likely to be affected by land use differences. The values of b' from the regressions for the high and low uplift zone channels overlap within 95% confidence bounds at $b' = 0.37–0.38$ (Fig. 4). These regressions also yield similar values of k'_w and width at the reference drainage area, suggesting that the valley

width data, although scattered, are not significantly different between different uplift rate zones. In the LUZ, the regressions for Juan and Hardy Creeks are quite different (with the parameters for Juan Creek more similar to the other study-area streams) and better constrained ($R^2 = 0.60$). This might again reflect land use differences, particularly because of in-channel railroad construction in Hardy Creek, but we have no basis to say this with certainty. At the southern end of the HUZ, Gitchell Creek is proportionally somewhat wider and has a lower value of b' than the other HUZ channels, with a regression similar to Hardy Creek (Table 3). The only discernible difference in
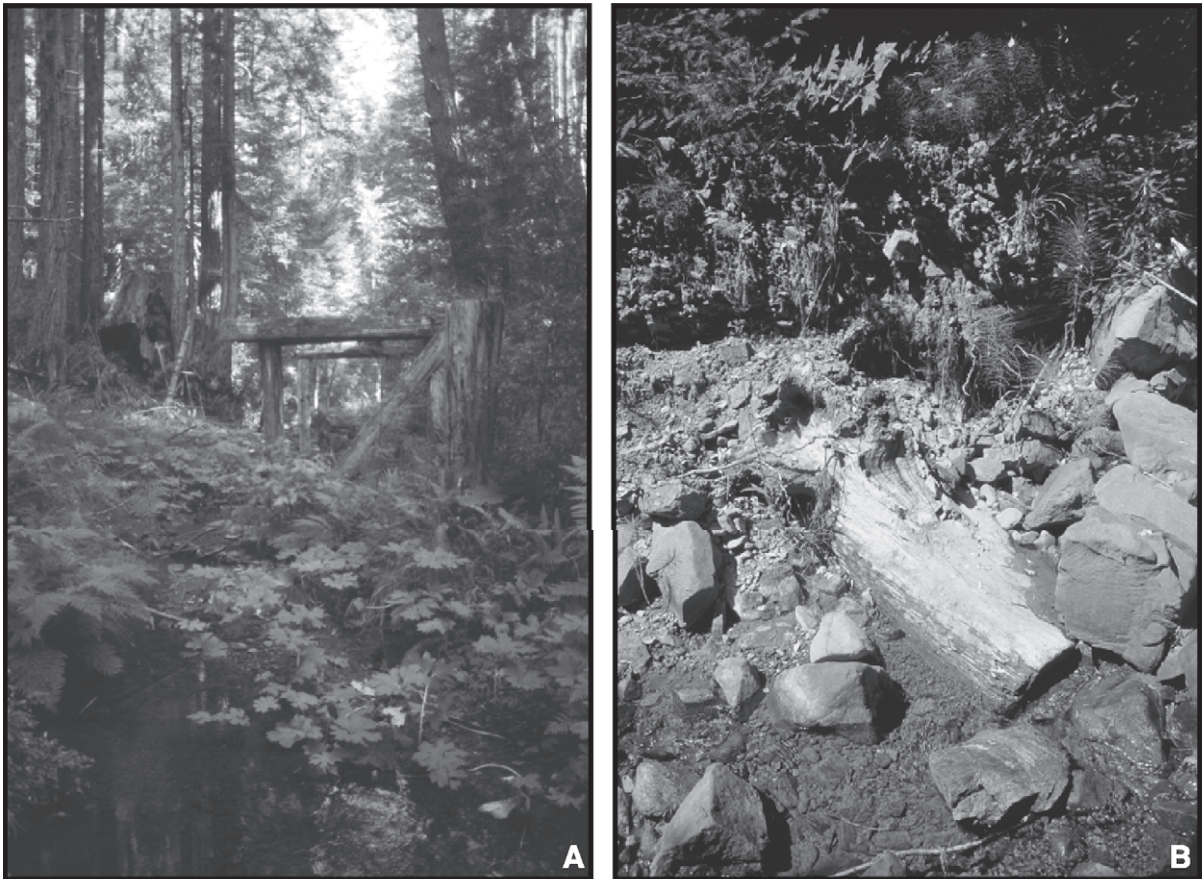
Fig. 5. Low uplift zone land use pictures. (A) Ruins of train trestles in the channel of Hardy Creek. (B) A partially buried cut tree stump in a 1.5-m-high river-right fill terrace in Juan Creek.

channel morphology for this stream was the presence of large (1–3 m diameter) sandstone boulders, which were not seen as extensively in adjacent drainages (Fig. 6). These boulders are sourced from the ridge to the east of the creek, a different unit from that of the rest of the studied channels (McLaughlin et al., 2000). We can offer no speculation as to how this might explain the apparently anomalous valley width data of Gitchell Creek.

Taking the width regressions as a whole, we use a value of b' of 0.4 for subsequent calculations, because this value is representative of most of the valley width measurements and the high-flow width measurements least affected by land use (Oat, Kinsey, and Shipman Creeks). This is in contrast to the preliminary results presented in our previous paper ($b' = 0.46 – 0.67$,

Snyder et al., 2000). We also are unable to discern any important difference in valley width between the uplift rate zones, so we believe that assuming k'_w as constant throughout the study area is acceptable.

4.3. Lithologic resistance

4.3.1. Background

The coefficient relating excess shear stress to incision rate (k_e, Eqs. (1) and (2)) depends on fluvial incision process, lithologic resistance, and possibly sediment flux. Here, we assume that incision processes are constant throughout the area, so that they do not contribute to variations in k_e. We consider the role of sediment flux in the next section. The possibility of systematic variations in lithologic resistance

Fig. 6. Massive, abraded sandstone boulders armoring the bed of Gitchell Creek.

to erosion must be considered through the use of careful field analysis. Since measurable bedrock incision by rivers occurs over long periods of time and/or during large events, we cannot make empirical estimations of the value of k_e directly. We can, however, search for evidence of important variations in lithologic resistance that would contribute to changes in k_e throughout the study area. For simplicity and brevity, we assume that changes in k_e due to lithology would also yield changes in critical shear stress (τ_c). Our analysis focuses on the former but can be expected to apply equally well to the latter.

Lithology clearly plays an important role in setting bedrock incision rates (Wohl, 1998; Stock and Montgomery, 1999; Whipple et al., 2000a,b). Bedrock in the study area is entirely within the Cretaceous–Tertiary Coastal Belt of the Franciscan Complex, a highly sheared and folded mix of argillite and sandstone with some conglomerate and igneous rocks (Jennings and Strand, 1960; Strand, 1962; McLaughlin et al., 2000). Broadly speaking, resistance varies locally, but overall the rocks are fractured and weak. From detailed aerial photographic interpretation and mapping of rocks in the HUZ of the King Range terrane, McLaughlin et al. (2000) divided the lithologies of the area into discrete zones

based on hillslope morphology. Similar aerial photographic interpretation has been done by Ellen for the region south of the McLaughlin et al. study area, including the basins of the LUZ (S. Ellen, unpublished mapping, USGS 1:100,000-scale Covelo Quadrangle). For the most part, the HUZ channels lie in the zone dominated by argillite with "irregular [hillslope] topography, lacking a well-incised system of sidehill drainages" (McLaughlin et al., 2000), while the high-relief King Range crest area (upper parts of Big, Big Flat, and Shipman Creeks, Fig. 1) is in the category of hillslope morphology characterized by "sharp-crested topography, with a regular, well-incised system of sidehill drainages." The LUZ channels generally lie in a zone characterized by hillslope morphology similar to the latter case (Ellen, unpublished mapping).

4.3.2. Methods

Here, we use detailed measurements of rock mass strength and jointing of channel bedrock outcrops to assess whether important variations in rock resistance can be found. To first order, lithologic resistance depends on two related factors: (i) intact rock mass strength and (ii) degree of fracturing due to weathering and jointing (Selby, 1993). Both of these factors

can be estimated in the field. To assess rock resistance in the field, we use two techniques: (i) Schmidt hammer measurements of rock mass strength and (ii) visual estimates of characteristic joint spacing. Our analysis of the former includes statistical tests of various sample subsets.

Mass strength of intact rock can be measured in the field with a Schmidt hammer (Selby, 1993). Because measurements near fractures are highly variable and difficult to treat in a quantitative way, we attempted to limit our survey to outcrops large enough to provide at least 10 different measurements of intact rock. We reported our data in Schmidt hammer R units, uncorrected for inclination of the hammer. We neglected this correction because we found that the correction is small ($<4R$ units) compared with the scatter inherent in the data. We omitted measurements $<11R$ units (10 is the minimum reading) and those that are clearly influenced by fractures in the rock (generally identified by hollow-sounding impacts). During our field surveys of channel morphology, we made Schmidt hammer measurements at stations spaced ~ 100 m apart, where outcrop permitted. At most stations, we took 25–50 readings. We then compared these measurements both within a basin and between zones within the field area.

Schmidt hammer measurements from channels in different settings can be compared through statistical analysis after some data reduction. Because we took different numbers of readings at each station, we compared mean values of each station, creating samples of basin-wide station-mean values. To assess rock mass strength of basins and zones as a whole, we compiled histograms of the mean values for each station. When looking at basin-wide data, we included

only readings from bedrock in channels likely to be dominated by fluvial processes; so, as with other analyses, we worked only with data from locations with $A>0.1$ km². The station mean values were also subdivided into those at locations with distinct bedrock steps (small waterfalls or knickpoints at least 0.5 m high) and those without bedrock steps. We tested the hypothesis that two samples are from the same distribution using Kolmogorov–Smirnov nonparametric methods (Davis, 1986; Rock, 1988), with the criteria that the hypothesis can be rejected if $p<0.05$. The Kolmogorov–Smirnov test is useful because it does not require that the two samples come from normal distributions (Davis, 1986; Rock, 1988). To look at intrabasin variability, we plotted Schmidt hammer means, maxima, and standard deviations along profiles. We also separated out stations at bedrock steps or knickpoints ≥ 0.5 m high to test whether these features were formed on disproportionally harder lithologies.

Our analysis of the degree of jointing consisted of visual estimates of the range of joint spacing in each outcrop. The goal of this methodology was simply to get an idea of the size of blocks that could be created by erosion of the bedrock. This technique is qualitative and not sufficient to characterize the overall contribution to lithologic resistance due to weathering and jointing. Nonetheless, we included our observations in the results presented here because they give at least a rough idea of the degree of fracturing of the rock throughout the study area.

4.3.3. Results

The basin-wide Schmidt hammer data are presented in Table 4. As with the channel width data,

Table 4
Schmidt hammer results from study area stations

Creek	All stations			Bedrock steps ≥ 0.5 m		No bedrock steps	
	Number	Mean $\pm 1\sigma$	Mode	Number	Mean $\pm 1\sigma$	Number	Mean $\pm 1\sigma$
Oat	30	49.7 ± 10.3	52.5	10	55.3 ± 6.8	20	46.9 ± 10.7
Kinsey	23	48.5 ± 8.9	42.5, 57.5	4	59.1 ± 3.9	19	46.3 ± 8.0
Gitchell	33	44.9 ± 10.5	47.5	5	50.7 ± 12.3	28	43.8 ± 10.1
High uplift zone	86	47.5 ± 10.1	57.5	19	54.9 ± 8.3	67	45.4 ± 9.7
Horse	31	41.8 ± 11.4	52.5	8	51.9 ± 3.2	23	38.2 ± 11.1
Hardy	26	43.1 ± 6.4	42.5	12	46.0 ± 7.0	14	40.6 ± 4.9
Juan	44	45.3 ± 7.5	47.5	8	48.3 ± 5.7	36	44.7 ± 7.8
Low uplift zone	70	44.5 ± 7.2	42.5	20	47.0 ± 6.4	50	43.5 ± 7.3

we focus on the pooled data for the HUZ and the LUZ, which increases sample size (Fig. 7; Table 4). The Schmidt hammer R mean value for the HUZ is 47.5 ± 10.1 (all errors are 1σ unless otherwise noted), and the LUZ is $44.5 \pm 7.2R$. Comparing the pooled samples from the LUZ and HUZ, the Kolmogorov–Smirnov (K–S) test indicates that we must reject the hypothesis that they are from the same distribution, indicating that there is a statistical difference ($p = 2.5 \times 10^{-4}$) between the rock-mass strength in the two uplift rate zones (Fig. 7A–B). Plots of Schmidt hammer maxima, mean, and standard deviation at each station along a channel show that outcrops have fairly random, variable resistance (Figs. 8B–10B).

In the HUZ, the stations located at bedrock steps ≥ 0.5 m yield a mean value of $54.9 \pm 8.3R$ (Figs. 7 and 8; Table 4). This mean is compared to a mean of $45.4 \pm 9.7R$ for stations without significant bedrock steps. A K–S test indicates that the hypothesis that these samples are from the same distribution can be rejected ($p = 2.7 \times 10^{-4}$). In the LUZ, the stations with a bedrock step have a mean of $47.0 \pm 6.4R$, and those without steps have a mean of $43.5 \pm 7.3R$. Here, the K–S test suggests that these samples may be from the same distribution ($p = 0.149$).

Basin-wide joint spacing calculations indicate mean minimum spacings of 2–3 cm in the HUZ and 4–5 cm in the LUZ and mean maximum spacings of 20–28 and 46–49 cm, respectively (Table 5; Figs. 8C–10C). Horse Mountain Creek, between the uplift rate zones, has a mean joint spacing range of 2–17 cm.

4.3.4. Interpretations

The Schmidt hammer data indicate that rocks of the HUZ are slightly harder than those of the LUZ, with a higher mean and mode (Table 4; Fig. 7). However, the difference in means is small, as the standard deviations overlap considerably. Conversely, the joint spacing data indicate that the HUZ rocks are somewhat more fractured than LUZ rocks (Table 5; Figs. 8C–10C). This is broadly consistent with the model proposed by Miller and Dunne (1996) that valley bottoms in areas of greater relief should be more fractured simply because of topographic perturbations of the stress field. However, we have not made the required systematic measurements of joint

spacing and orientation to test their hypothesized feedback between relief production and bedrock fracturing.

Separating the Schmidt hammer station data into samples at ≥ 0.5 m bedrock steps and those not at steps shows that the knickpoints in the HUZ are controlled by areas of particularly resistant rock, with a significantly different distribution and greater sample mean (Fig. 7D and F; Table 4). This is not the situation in the LUZ, where the bedrock step sample is only slightly harder than the nonstep sample (Fig. 7C and E; Table 4). This difference may be related to the increased erosion rates of the HUZ, which might (i) emphasize the importance of zones of more resistant rock as a channel responds to higher rates of rock uplift and/or (ii) give less opportunity for preparation and fracturing of bedrock by weathering. Alternatively, this difference may be a reflection of the somewhat greater distribution of resistant (high mean R value) areas of rock in the HUZ, which is clearly indicated by the left-skewed appearance of the histograms for the overall HUZ sample (Fig. 7B) and bedrock step HUZ sample (Fig. 7D). This suggestion is supported by the observation that the nonbedrock step HUZ sample is more similar to the LUZ samples in that it has a lower mean and is less skewed (Fig. 7F). In any case, zones of resistant rock appear to play an important role in controlling the location of channel knickpoints, particularly in the HUZ.

Unfortunately, none of our channel surveys cross any of the significant hillslope morphologic contacts mapped by McLaughlin et al. (2000) or Ellen (unpublished), so we cannot assess the importance of these potential intrabasin variations in hillslope morphologic expression. However, we can say that the gradients of stream channels that cross these transitions in the King Range (Big, Big Flat, and Shipman Creeks) do not seem to be affected by this change in hillslope morphology (Snyder et al., 2000). We also can speculate that the differences we observe in mass strength (greater in the HUZ) and joint spacing (greater in the LUZ) could be broadly consistent with the mapping by McLaughlin et al. (2000) and Ellen (unpublished), which put these channels in different hillslope morphology zones.

Importantly, the lower, south-flowing part of Horse Mountain Creek follows a major shear zone (McLaughlin et al., 2000). This shear zone is on strike
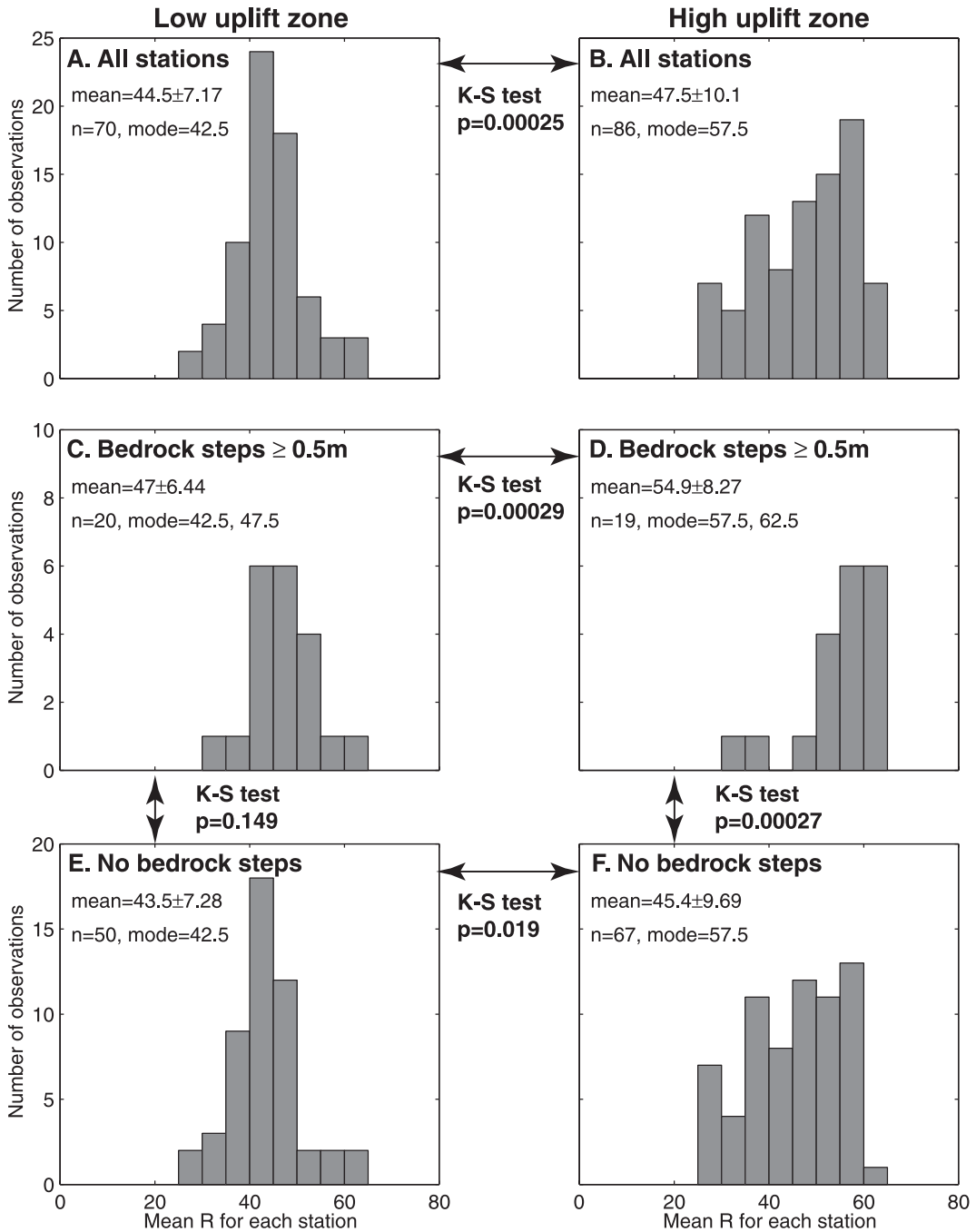
Fig. 7. Histograms of Schmidt hammer data for mean values of each station in the low uplift zone (left column) and high uplift zone (right column). Also shown are sample mean values with associated 1σ error bounds; number of measurements in each sample; and sample modes. Arrows indicate the probability that adjacent pairs of samples are from the same distribution based on a Kolmogorov–Smirnov (K–S) test. (A–B) All data. (C–D) Data for stations at bedrock steps in the channel >0.5 m high. (E–F) Data for stations not at bedrock steps. See Table 4 for data from individual streams.
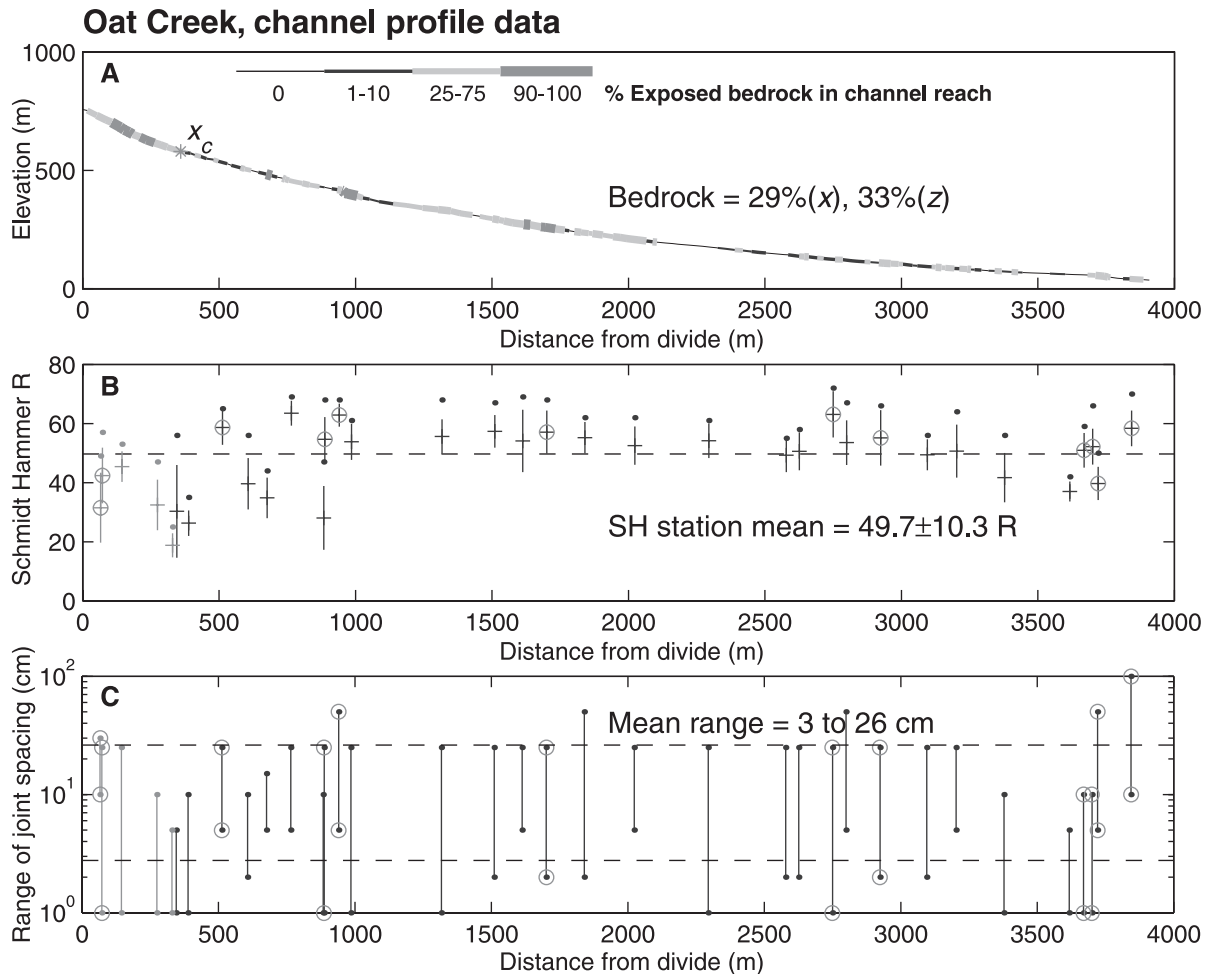
Fig. 8. Channel profile data for Oat Creek in the high uplift zone. (A) Percent of each channel reach that is exposed bedrock outcrop. The place in the channel where $A = 10^5$ m^2 is denoted by x_c. Bedrock percentage includes only the part of the channel below x_c. (B) Schmidt hammer mean values (crosses), 1σ error bounds (lines), and maxima (dots) for each station. Overall mean value is marked by horizontal dashed line. (C) Visual estimates of the range of joint spacing at each station; dashed lines indicate mean range. *Y*-axis has a logarithmic scale. (B–C) Circles indicate stations at bedrock steps >0.5 m. Grey data are those in the channel above x_c.

with and just north of the mapped active trace of the San Andreas Fault (Fig. 1; Prentice et al., 1999). Channel slopes in this area are anomalously low (Snyder et al., 2000). This zone is characterized by particularly fractured rocks with a corresponding decrease in rock mass strength and joint spacing (Fig. 10). Relatively little data could be collected in this area because of a paucity of outcrops of sufficient size and competence for Schmidt hammer measurements. Joint spacings in the 1.5-km section of channel near the mouth of Horse Mountain Creek are consistently in the 1–10 or 1–5

cm categories (Fig. 10C); and station mean Schmidt hammer *R* values are around 30, well below the basin-wide average of 41.8. These observations confirm that the analysis is capable of picking up important, systematic variations in rock resistance.

The central question of the analysis of lithologic resistance can be stated as follows: are there systematic differences between rocks of the HUZ and LUZ that could affect the values of k_e and τ_c? One interpretation of the Snyder et al. (2000) analysis is that rocks of the HUZ might be more easily eroded than rocks of the
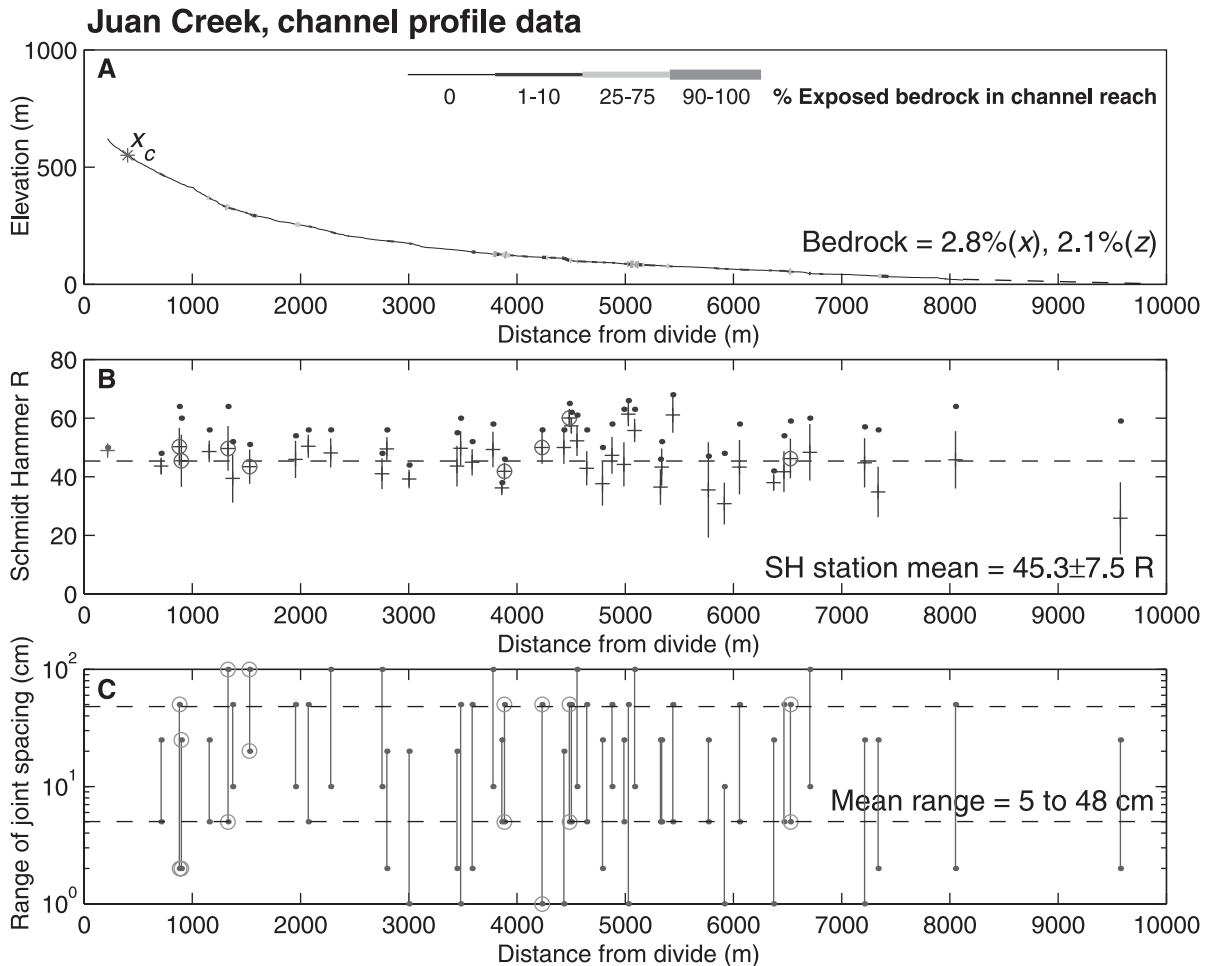
Fig. 9. Channel profile data for Juan Creek, in the low uplift zone. See Fig. 8 for description. (A) Area not included in the field survey marked by dashed line.

LUZ, yielding more efficient incision processes (higher k_e and K). The jointing data are consistent with this situation, but the data on rock-mass strength are not. The latter data are clearly more robust than the jointing data; and they suggest that, if anything, rocks within the HUZ are (at least locally) harder and therefore presumably more difficult to erode (lower k_e). We cannot discern with certainty if either factor is significantly affecting incision rates throughout the study area. Because the analysis presented here does not provide evidence for what we might suspect to be major differences in mass strength or jointing, however, we proceed with the assumption that k_e and τ_c do not vary due to variations in rock resistance.

4.4. Channel-bed morphology

4.4.1. Background

Sediment flux is likely to be an important control on the ability of a stream to incise its bed and, hence, on possible rates of incision. Sklar and Dietrich (1998) proposed a model for stream incision by particle (sediment) impacts on the bed. In their model, low sediment flux give rise to a "tool-starved" condition with insufficient impacts to break apart and transport channel bedrock. At the other end of the spectrum, sediment flux greater than transport capacity buries the channel bedrock, reducing erosion rates to include only rare, catastrophic events that can
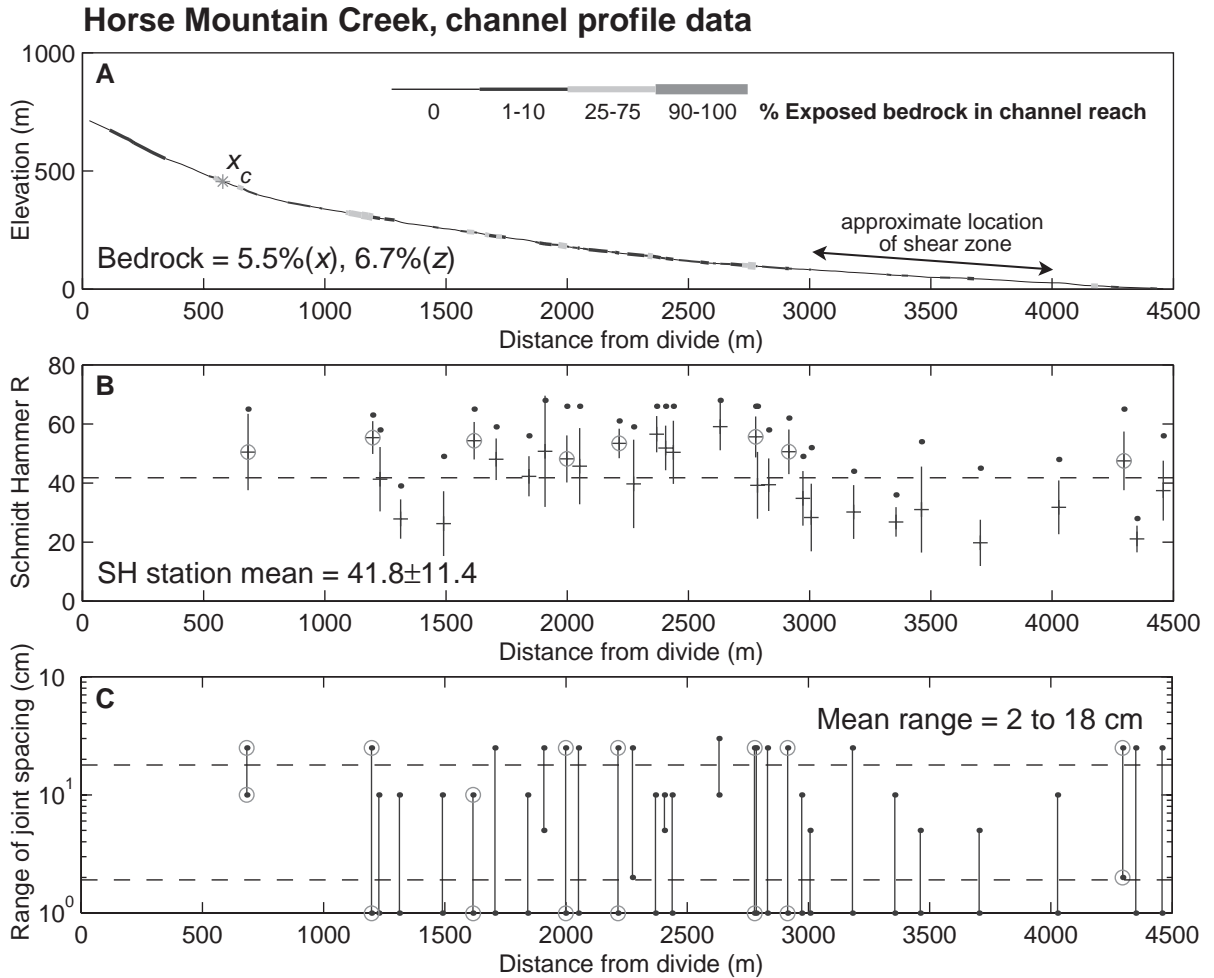
Fig. 10. Channel profile data for Horse Mountain Creek in the intermediate uplift zone. See Fig. 8 for description. (A) Arrow indicates the section of the channel oriented along a major shear zone.

move the bed material. This gives rise to transport-limited incision or depositional conditions. In between these two cases is a situation where an optimal sediment flux yields the most effective bedrock incision. On an intuitive level, this simple presentation of the Sklar and Dietrich argument is likely to be correct, so the question becomes: is this effect important in this field setting? For the purposes of this paper, we propose that sediment flux through the channel might influence the value of k_e (Eq. (2); Whipple and Tucker, 1999).

In our previous paper (Snyder et al., 2000), we argued that the main-trunk channels of the study area

are likely to be eroding at the same rate that the land surface is uplifting. We are less confident, however, about the response of tributaries and hillslopes. Throughout the study area, and particularly in the HUZ, we see inner gorges and "hanging" tributaries that have a pronounced convexity at their junction with the main channel (Snyder et al., 1999). These observations suggest the possibility that the main channels might have been more rapid in their response to increased rock uplift rates than the channels throughout the rest of the basins. Put simply, we are not confident that the steady-state model we believe applies to the main channels is appropriate for the

Table 5
Channel bedrock and joint spacing results

Creek	Channel bedrock (%)		Joint spacing (cm)	Notes
	Horizontal	Vertical		
Oat	29	33	3−26	
Kinsey	78	76	1−31	top survey
	12	17	no data	bottom survey
	20	33		overall
Gitchell	3.6	5.3		top survey
	4.5	4.2	2−21	bottom survey
	4.3	4.8		overall
Horse	5.5	6.6	2−18	
Hardy	5.0	9.5	4−43	
Juan	2.8	2.1	5−48	

entire drainage basins. Therefore, although we might assume that the steeper hillslopes and tributaries of the HUZ indicate greater sediment flux out of the system than the LUZ, we cannot say this with any quantitative confidence.

We are left with taking an essentially qualitative approach to the problem of sediment flux by making observations of the present morphology of the channel bed throughout the study area. We suggest two cases for how the value of k_e might be affected by sediment flux. First, if the bed is mostly covered by alluvium, sediment flux rate might slow incision rates because bed load impact energy would be spent reducing the size of bed sediment, not incising bedrock. Conversely, if the bed is composed mostly of exposed bedrock outcrop, then either sediment flux is enhancing bedrock incision or is playing a small role in setting bedrock incision rates. In the first situation, k_e is likely to be reduced because of increased sediment flux. In the second case, the value of k_e will either be unaffected by sediment flux or be increased.

4.4.2. Methods

During our field surveys, we made detailed observations of the stream morphology, including channel-type classification (Montgomery and Buffington, 1997); size and source (alluvial or colluvial) of bed sediment; size, type and distribution of terraces; and the presence of bedrock outcrops. As we surveyed each ~ 25-m reach of channel, we made visual assessments of the percentage of the bed and sidewalls that was composed of exposed bedrock. Each reach fell into one of eight categories: 0% for no exposed

bedrock; 1% for a trace; 10%, 25%, 50%, 75%, or 90% for varying degrees of exposure; and 100% for bedrock channel with no continuous sediment deposits. These values were plotted on the channel longitudinal profiles and integrated in the horizontal (distance, x) and vertical (elevation, z) directions to calculate an overall percentage of channel bedrock for the fluvial part of the system (A>0.1 km^2). Although this technique is only semiquantitative, it does provide a relative measure of the channel morphology to allow interbasin comparison.

4.4.3. Results

Horizontally integrated channel bedrock ranges from 2.6% to 2.7% in Gitchell and Juan Creeks to 27% in Oat Creek (Figs. 8A–10A; Table 5). For integration in the vertical direction, bedrock percentages range from 2.0% in Juan Creek to 31% in Oat Creek. Plots of channel bedrock percentage along the stream profiles show that outcrops are distributed throughout the channels, with perhaps a slightly increased percentage in the upper half of the profiles (Figs. 8A–10A).

4.4.4. Interpretations

In five of the six channels studied, the percentage of channel bedrock is greater in the vertical integration than the horizontal (Table 5). This simply shows that, in general, bedrock channel segments are steeper than sediment-mantled segments. The wide distribution of bedrock outcrops throughout the channels indicates that any alluvial cover is a thin mantle (<3 m) and reinforces the interpretation that the longitudinal profiles of these streams are controlled by their ability to incise bedrock (Figs. 8A–10A; Snyder et al., 2000).

In general, HUZ channels have more exposed bedrock than LUZ channels (Table 5). This is particularly true when Oat and Kinsey Creeks are compared to Hardy and Juan Creeks. Gitchell Creek seems to have an anomalously low percentage of exposed bedrock, reflecting the large sandstone boulders that make up the channel bed material in many places (Fig. 6). These boulders might effectively act as bedrock for this channel, with incision limited by the ability of the channel to detach pieces from them. The boulders might have an effect on channel width and bedrock in Gitchell Creek, but they do not appear to affect the

longitudinal profile, which is consistent with adjacent HUZ creeks (Snyder et al., 2000). We set aside Gitchell Creek in order to address the general trend that HUZ channels have much more exposed bedrock than LUZ channels.

Taken at face value, these data suggest that the LUZ channels are in a situation where incision is limited by bed protection from sediment cover (suggesting a low value of k_e) or perhaps even transport-limited conditions. At the same time, the HUZ channels appear to have ample opportunity to erode bedrock, not limited by their sediment flux rate (presumably somewhat higher in the long term). However, as with the channel width signal, the land use differences between the two areas are likely to play an important role in setting the present-day channel morphology. The LUZ channels clearly show signs of a recent period of high sediment flux due to activities related to timber harvesting (Fig. 5). The ubiquitous young (< 100 years old) fill terraces of Hardy and Juan Creeks indicate that the main channels are trenching actively through this sediment. This recent signal is likely the dominant control on bed morphology in the LUZ. In fact, if we consider the possibility that the recent pulse of sediment has yielded a greater short-term sediment flux rate in the LUZ than in the HUZ, then the LUZ is presently an example of bedrock incision limited by an overabundance of sediment. However, this is likely a short-term perturbation; and in the absence of comparable HUZ and LUZ channel morphologies, we are unable to make any inferences about the role of sediment flux as a response mechanism.

To summarize, although a model for k_e changing as a function of sediment flux is plausible for this field area (Eq. (2)), we cannot draw any firm conclusions, because of land use differences. However, if no other cause of a change in k_e (or other factors) can explain the observed relationship between steady-state channel slope (S_e) and uplift rate (U; Eqs. (9) and (10); Snyder et al., 2000), then we might conclude that incision rate is dependent on the presumed long-term difference in sediment flux rate between the HUZ and LUZ. Conversely, if other plausible mechanisms can explain the $S_e - U$ data adequately (for instance τ_c), then perhaps sediment flux is not an important control on incision rates in this field area. The theoretical role of sediment flux in this field area is considered further by Snyder et al. (2003).

5. Discussion

5.1. Inferences about process transitions from channel width data

The full, divide-to-mouth channel width datasets paired with observations of channel morphology provide some insight into downstream process transitions (e.g., Dietrich et al., 1993). The width–drainage area scaling appears to break down at a drainage area of ~ 10^5 m^2 (0.1 km^2; Fig. 4). This is at the same value as the break in channel slope–drainage area observed by Snyder et al. (2000). In the field, this is typically the place where two ephemeral gullies come together, doubling the drainage area, to form a perennial stream (Fig. 11). Downstream from this junction, channel sediment and bedrock outcrops exhibit clear signs of fluvial reworking (organization into bed forms, and rounding and fluting, respectively), whereas these morphologies are rare in upstream gullies. We suggest that this break reflects the switch from colluvial-dominated (mostly debris flows; Stock and Dietrich, 1998, 2003) to fluvial-flood-dominated incision processes, although both sets of processes are certainly active in both areas. This scaling break is likely gradational. For a given stream the exact location of this transition is difficult to identify in the field. For this field area the break could be argued to occur between $A \approx 10^5$ m^2 and $A \approx 10^6$ m^2. However, the similarity in $W - A$ and $S - A$ scaling, along with field observations, suggests that $A \approx 10^5$ m^2 is an important transition.

The scaling break is observed most strongly in the HUZ channels (Fig. 4), which may be related to two factors. First, erosional rills and gullies (with thin veneers << 1 m of sediment stored in the channel) occupy the first 100–300 m downstream from the divide in the HUZ. This is generally not the case in the LUZ, where several hundred meters of rounded, convex-up hillslopes and intermittent sediment-filled colluvial hollows characterize ridge crests. Second, Hardy and Juan Creeks have numerous roads running on and just below the ridges, which greatly influence local channel morphology, often diverting flow out of ephemeral gullies. Both factors mean that in many cases data collection is impossible because the rills or gullies cannot be followed or are not defined enough to permit width measurement with any certainty in the

Fig. 11. Downstream process transitions in Kinsey Creek (high uplift zone). (A) Narrow (~ 2 m wide), ephemeral colluvial gully ~ 300 m from the divide ($A < 10^5$ m^2). (B) Bedrock channel plunge pool at the base of a 2-m-high waterfall ~ 1400 m from the divide ($A \approx 10^6$ m^2).

LUZ channels. This is reflected by the comparative lack of data from drainage areas less than about 2×10^4 m^2 (0.02 km^2) in the LUZ (Fig. 4). We surveyed upper tributaries in both Juan Creek and Hardy Creeks in an unsuccessful attempt to fill in this data gap (Table 3).

5.2. Channel concavity

Steady-state channel concavity is given by the area (A) exponent in Eqs. (9) and (10) $((\alpha/\beta)(c - b') = m/n$, hereafter m/n). Using slope–area regressions from longitudinal profile data, we found previously that the true mean channel concavity index (θ) of the 21 study area streams was 0.43 ± 0.22 (2σ) and that these streams were likely close to steady state

(Snyder et al., 2000). The large uncertainty in this estimate reflects the scatter inherent in power-law regressions over few orders of magnitude. Also, use of a less inclusive lower bound on drainage area for the fluvial part of the system in the regressions ($A > 10^5$ m^2) would have increased concavity estimates somewhat (although within error bounds), as discussed by Stock and Dietrich (1998, 2003). Using the empirical calibrations presented here ($c = 1$; $b' \approx 0.4$; Table 6), Eqs. (9) and (10) predict that the steady-state concavity index of these streams should be around 0.51. This calibrated theoretical value matches the previous empirical estimate of θ (from longitudinal profile data) within uncertainty, although it does suggest that the true concavity may be somewhat less than theory would predict. Previously, we

Table 6
Parameter values and units

Basic variables	
x [m]	streamwise horizontal distance from divide
x_c [m]	distance at $A = 10^5$ m^2
z [m]	vertical elevation above sea level
A [m^2]	drainage area
S	channel gradient
S_e	steady state channel gradient
Q [m^3 s^{-1}]	stream discharge
w [m]	channel width
E [m year^{-1}]	channel incision rate
U [m year^{-1}]	rock uplift rate
τ_b [Pa]	bed shear stress
k_w [m$^{(1-3b)}$s^b]	channel width–discharge coefficient
b	channel width–discharge exponent
m	drainage area exponent (Eq. (7))
n	slope exponent (Eq. (7))
m/n	theoretical steady-state channel concavity
θ	actual (empirical) channel concavity

Physical parameters	
$\alpha = 3/5$	exponent on (Q/w) quotient
$\beta = 7/10$	exponent on S
$\rho = 1000$ kg m^{-3}	density of water
$g = 9.8$ m s^{-2}	gravitational acceleration
$N = 0.07$ m$^{-1/3}$ s	Manning roughness coefficient (estimated; Barnes, 1967)

Empirically calibrated parameters	
$c = 1$	discharge–width exponent
$b' = 0.4$	width–drainage area exponent
$k'_w = 0.0215$ m$^{(1-2b')}$	width–drainage area coefficient

Reference slope–area data (for Fig. 12; from Snyder et al., 2000)	
$A_{ref} = 10^6$ m^2	reference drainage area
$U_1 = 0.0005$ m year^{-1}	low uplift zone rock uplift rate
$U_2 = 0.004$ m year^{-1}	high uplift zone rock uplift rate
$S_1 = 0.14$	low uplift steady state slope at A_{ref}
$S_2 = 0.24$	high uplift steady state slope at A_{ref}

Unknown parameters (cannot calculate unique values)	
τ_c [Pa]	threshold/critical shear stress
k_q [m s^{-1}]	discharge–drainage area coefficient (depends on a reference flood recurrence interval)
k_e [m year^{-1} Pa^{-a}]	shear stress–incision rate coefficient
a	shear stress–incision rate exponent

Derived parameters	
k_t [m$^{18/25}$ Pa]	shear stress coefficient (Eq. (5))
K [m$^{-1/35}$ year^{-1}]	coefficient of erosion (Eqs. (7) and (8))
$m/n = 0.51$	predicted channel concavity (Eqs. (7) and (8))

presented preliminary channel width data that was more consistent with $b = 0.6$, which provided a more satisfying match to the observed concavity (Snyder et al., 2000). However, the more complete investigation of channel width does not support this higher value of b'.

Although our empirically calibrated theoretical prediction for m/n is reasonably close to the observed value of θ, an investigation of the assumptions associated with this prediction is warranted. The basic premise of Eqs. (9) and (10) is that at steady state (and spatially constant U and K), the channel slope has adjusted so that excess shear stress (or shear stress, if $\tau_c = 0$) is constant downstream (Snyder et al., 2000). If the true concavity is less than the value predicted in Eqs. (9) and (10), this suggests that either shear stress is actually decreasing downstream or the derivation of Eqs. (2), (9) and (10) is incomplete or oversimplified. Here, we address a set of possible explanations, which could result from a variety of violations of the basic assumptions of Eqs. (9) and (10).

(i) The system may not be in steady state; for instance, a wave of incision could be migrating headward through the channels. This is conceivable, although we would expect a distinct break in the slope–area relationship that is not observed (Snyder et al., 2000).

(ii) The rock uplift rate (U) may not be constant throughout the basin. An increase in U downstream could explain the observed concavity (e.g., Kirby and Whipple, 2001), but the wide (≤ 1 km), flat emergent marine terraces in the northern and southern parts of the study area are not consistent with significant tectonic tilting (Merritts et al., 1992; Snyder et al., 2000). Differential motion along discrete faults crossing channels could also cause intrabasin changes in uplift rate; but no structures that would lead one to suspect this situation have been identified, except possibly the shear zone in Horse Mountain Creek (McLaughlin et al., 2000).

(iii) Downstream from the divide, the bed may be progressively buried and therefore protected by sediment, lowering the value of k_e. Most of the surveys are consistent with this possibility, with more bedrock exposed in the upper parts of the channels (Figs. 8A–10A).

(iv) Holocene eustatic sea-level rise might be causing some reduction in sediment-carrying capacity in the lower parts of the basin. This is most likely in the low uplift zone, where rock uplift rates are less than recent rates of sea-level rise. Indeed, these channels are more alluviated in the lower reaches (Fig. 9A); and for this reason, these areas were not included in the calculations of concavity from longitudinal profiles by Snyder et al. (2000).

(v) Intrabasin orographically driven gradients in precipitation might affect stream discharge in a way not captured by the analysis in Section 4.1. For example, c measured within individual study-area basis could be less than 1, corresponding to a reduction in the predicted concavity. The affect of orographic precipitation on concavity has been investigated by Roe et al. (2002).

(vi) Perhaps the most likely case is a downstream decrease in the hydraulic roughness parameter (in this case, N). For instance, if N varied from 0.070 $m^{-1/3}$ s at $A = 10^5$ m^2 to 0.048 $m^{-1/3}$ s at $A = 10^7$ m^2 this would translate into a relationship where N goes as $A^{-0.08}$; and m/n in Eqs. (9) and (10) would be 0.43, matching the value of θ. We present this calculation for heuristic purposes—to illustrate the point that minor downstream variations in channel roughness could explain the slight data mismatch. Variations in Manning's N on this order as the stream makes the transition from a steep mountain channel choked with woody debris and boulders delivered from mass wasting on adjacent hillslopes (i.e., $A = 10^5$ m^2), to a 10-m-wide, pool-riffle or plane-bed channel with well-formed smooth banks ($A = 10^7$ m^2) seems like a reasonable possibility, consistent with other field observations of downstream changes in morphology (Barnes, 1967; Richards, 1982; Montgomery and Buffington, 1997; Buffington and Montgomery, 1999). Unfortunately, we do not have the required field measurements of N to test this hypothesis.

5.3. The importance of critical shear stress

Most models of bedrock channel incision neglect the critical shear stress term (τ_c) in Eq. (1), and therefore use a form of Eq. (8) to describe channel evolution. Recently, Tucker and Bras (2000) used a

fluvial erosion model forced by a stochastic distribution of storms to show that in the absence of a threshold term, for reasonable (<2) values of a, the highest erosion rates occurred in the least variable climatic conditions—i.e., constant gentle rain. This is in direct opposition to the basic assumption usually used to justify ignoring the τ_c term—that the big storms do most of the work and produce shear stresses that far exceed τ_c. This observation spurred our initial interest in investigating the role of the threshold shear stress term. The role of erosion thresholds is studied in depth by Snyder et al. (2002).

A cursory comparison of Eqs. (9) and (10) reveals that nonzero values of τ_c influence the expected relationship between steady-state slope (S_e) and rock uplift rate (U). To illustrate, we consider S_e at a reference drainage area ($A_{ref} = 10^6$ $m^2 = 1$ km^2; Fig. 12; Table 6), which is equivalent to, but more intuitive than, the comparisons using the channel steepness index (Snyder et al., 2000, 2002). We use the mean cases from the longitudinal profile analysis in Snyder et al. (2000) for values of S_1 and S_2, the slopes at A_{ref} for the LUZ and HUZ, respectively. When $\tau_c = 0$ is assumed (Eq. (10)) with $n = 1$ (erosion rate linear in slope; $a = 10/7$), steady-state slope varies linearly with uplift rate (U). In our previous analysis (Snyder et al., 2000), we found that one value of K cannot match the observed relationships between slope and uplift rate for both the LUZ and HUZ (unless n ≈ 4), implying that K must vary between the zones (Fig. 12). However, simply the presence of the nonzero τ_c term in Eq. (9) makes the relationship between S and U nonlinear, and K need not vary to explain the data (Fig. 12).

Unfortunately, an infinite set of combinations of τ_c, k_e, and k_q can explain the data (for any given value of a or n), so we are unable to place constraints on these key unknown parameters. The model presented here assumes the existence of a dominant erosive flood event of unknown magnitude (parameterized by k_q). For any value of k_q, a corresponding value of τ_c can be found. A minimum value of τ_c would be the Shields shear stress required to move the larger blocks of sediment (20–30 cm in diameter, similar to typical joint spacing) observed on the bed (100–300 Pa). However, we cannot further constrain this value with the present model. The approach of Tucker and Bras (2000) presented a solution to this problem because using a stochastic distribution of storms eliminates the
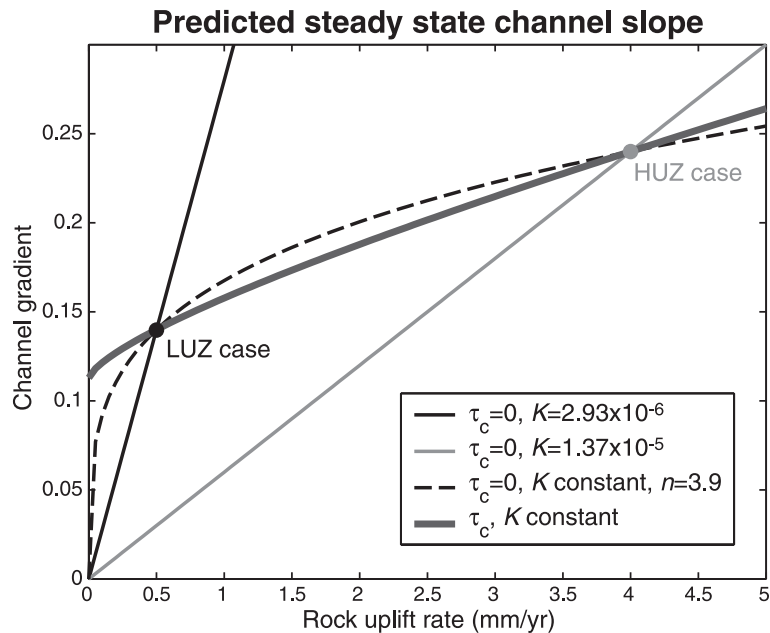
Predicted steady state channel slope

Fig. 12. Predicted steady state channel gradient (S_e) at $A = A_{ref} = 10^6$ m^2 vs. rock uplift rate for several models. Circles denote mean values for the HUZ and LUZ based on longitudinal profile data from Snyder et al. (2000). Fine, solid black line is the Eq. (10) case with $n = 1$ for a LUZ channel; fine, gray line is for a HUZ case. Dashed, black line is the solution to Eq. (10) to match both data points with a constant value of K. Thick, black line is a solution to Eq. (9) to match both data points with a constant value of K and τ_c. See Table 6 for parameter values used in these curves.

need to assume a dominant discharge (k_q), thereby allowing back calculation of τ_c and k_e, as was done for the Mendocino triple junction field area in a parallel study (Snyder et al., 2003). In the analysis presented here, we conclude only that a nonzero threshold shear stress for incision provides a plausible alternative to systematic variations in k_e.

6. Conclusions: channel response to tectonic forcing

The streams of the Mendocino triple junction region offer the opportunity to look at the effects of a major change in rock uplift rate. We evaluate the responses of fluvial systems to this change, with specific reference to how these changes will affect the shear-stress-model parameters. We find that the most important difference between the HUZ and LUZ watersheds is the increased stream discharge in the HUZ due to orographic enhancement of precipitation by higher mountains. Comparison of discharge

records from Honeydew Creek just east of the HUZ to gaging station data from throughout the region, indicates that Honeydew Creek receives about twice as much flow as the rest of region corresponding to a likely twofold increase in the value of k_q, less than the value assumed by Snyder et al. (2000).

Land use differences between the HUZ and LUZ limit our ability to assess potential changes in channel width and the role of sediment flux. As a partial solution to this problem, we emphasize our valley-width data, for this is likely to be less affected by land use. Our analysis of channel-width data is consistent with assuming that k_w' and b' are constant throughout the study area. We cannot directly say anything conclusive about the importance of sediment flux in controlling incision rate. This situation provides a nice illustration of the importance of the time scale of response to perturbations. Because of higher uplift rates over the past $\sim$ 100 ka, we expect narrower channels in the HUZ. However, most likely because of a sediment pulse in the past $\sim$ 100 years, we observe narrower high-flow channels in the LUZ. The same is true of

channel morphology. We might expect the onset of high hillslope erosion rates, responding to stream incision, to begin to bury the HUZ channels in alluvium. However, we see this situation in the LUZ, again because of a recent, short-term perturbation in sediment flux.

Our analysis of channel bedrock outcrops indicates that rocks of the HUZ have slightly greater mass strength than those of the LUZ but are also somewhat more fractured. Therefore, we conclude that k_e and τ_c are likely to be approximately constant throughout the study area.

Previously, we placed constraints on the value of n for the case where $\tau_c = 0$ (Eq. (8); Snyder et al., 2000). The data presented here does not significantly change this analysis; we have no evidence for changes in K other than the variation in discharge ($k_{q1}/k_{q1} = 1/2$; Table 6), which suggests that a model with $n = 1.5–2.3$ can explain the data. However, we hasten to point out that we now believe this analysis to be oversimplified because values of $\tau_c > 0$ significantly change the model prediction for steady-state channels, and can explain the $S–U$ data without appealing to unexplained variations in other parameters, particularly k_e. Because we have little knowledge of what value of τ_c (or k_q) is appropriate for the study area, we are unable to place any additional constraints on the values of n or a. Further work on the importance of threshold shear stress in bedrock channel incision is needed to more fully calibrate the model.

Acknowledgements

References

Baker, V.R., Kale, V.S., 1998. The role of extreme floods in shaping bedrock channels. In: Tinkler, K.J., Wohl, E.E. (Eds.), Rivers Over Rock: Fluvial Processes in Bedrock Channels. Geophysical Monograph, vol. 107. American Geophysical Union, Washington, pp. 153–165.

Barnes, H.H., 1967. Roughness Characteristics of Natural Channels. U.S. Geological Survey Water-Supply Paper, vol. 1849. 213 pp.

Barros, A., Lettenmaier, D., 1993. Dynamic modeling of orographically induced precipitation. Reviews of Geophysics 32, 265–284.

Buffington, J.M., Montgomery, D.R., 1999. Effects of hydraulic roughness on surface textures of gravel-bed rivers. Water Resources Research 35 (11), 3507–3521.

Davis, J.C., 1986. Statistics and Data Analysis in Geology. Wiley, New York. 646 pp.

Dietrich, W.E., Wilson, C.J., Montgomery, D.R., McKean, J., 1993. Analysis of erosion thresholds, channel networks, and landscape morphology using a digital terrain model. Journal of Geology 101, 259–278.

Dunne, T., Leopold, L.B., 1978. Water in Environmental Planning. Freeman, New York. 818 pp.

Hack, J.T., 1973. Stream profile analysis and stream-gradient index. Journal of Research of the U.S. Geological Survey 1 (4), 421–429.

Hamilton, L.C., 1992. Regression With Graphics: A Second Course in Applied Statistics. Wadsworth, Belmont, CA. 363 pp.

Hancock, G.S., Anderson, R.S., 2002. Numerical modeling of fluvial terrace formation in response to oscillating climate. Geological Society of America Bulletin 114, 1131–1142.

Harbor, D.J., 1998. Dynamic equilibrium between an active uplift and the Sevier River, Utah. Journal of Geology 106 (2), 181–194.

Howard, A.D., 1994. A detachment-limited model of drainage basin evolution. Water Resources Research 30, 2261–2285.

Howard, A.D., Kerby, G., 1983. Channel changes in badlands. Geological Society of America Bulletin 94, 739–752.

Jennings, C.W., Strand, R.G., 1960. Geologic Map of California, Ukiah Sheet. Department of Conservation, State of California, Sacramento, CA.

Kirby, E., Whipple, K.X., 2001. Quantifying differential rock-uplift rates via stream profile analysis. Geology 29 (5), 415–418.

Lavé, J., Avouac, J.P., 2000. Active folding of fluvial terraces across the Siwaliks Hills, Himalayas of central Nepal. Journal of Geophysical Research 105 (B3), 5735–5770.

Leopold, L.B., Maddock Jr., T., 1953. The Hydraulic Geometry of Stream Channels and Some Physiographic Implications. U.S. Geological Survey Professional Paper, vol. 252. Washington, DC.

Leopold, L.B., Wolman, M.G., Miller, J.P., 1964. Fluvial Processes in Geomorphology. Freeman, San Francisco, CA. 522 pp.

McLaughlin, R.J., et al., 2000. Geology of Cape Mendocino, Eureka, Garberville, and Southwestern Part of the Hayfork 30 × 60 Minute Quadrangles and Adjacent Offshore Area, Northern California. U.S. Geological Survey Miscellaneous Field Studies MF-2336, Washington, DC.

Merritts, D.J., 1996. The Mendocino triple junction: active faults, episodic coastal emergence, and rapid uplift. Journal of Geophysical Research 101 (B3), 6051–6070.

Merritts, D., Bull, W.B., 1989. Interpreting Quaternary uplift rates at the Mendocino triple junction, northern California, from uplifted marine terraces. Geology 17, 1020–1024.

Merritts, D., Vincent, K.R., 1989. Geomorphic response of coastal streams to low, intermediate, and high rates of uplift, Mendocino junction region, northern California. Geological Society of America Bulletin 101, 1373–1388.

Merritts, D.J., Chadwick, O.A., Hendricks, D.M., Brimhall, G.H., Lewis, C.J., 1992. The mass balance of soil evolution on late Quaternary marine terraces, northern California. Geological Society of America Bulletin 104, 1456–1470.

Miller, D.J., Dunne, T., 1996. Topographic perturbations of regional stresses and consequent bedrock fracturing. Journal of Geophysical Research 101 (B11), 25523–25536.

Montgomery, D.R., Buffington, J.M., 1997. Channel-reach morphology in mountain drainage basins. Geological Society of America Bulletin 109 (5), 596–611.

Montgomery, D.R., Gran, K.B., 2001. Downstream hydraulic geometry of bedrock channels. Water Resources Research 37 (6), 1841–1846.

Paola, C., Heller, P.L., Angevine, C.L., 1992. The large-scale dynamics of grain-size variation in alluvial basins: 1. Theory. Basin Research 4, 73–90.

Parker, G., Izumi, N., 2000. Purely erosional cyclic and solitary steps created by flow over a cohesive bed. Journal of Fluid Mechanics 419, 203–238.

Pazzaglia, F.J., Wegmann, K., Garcia, A.F., 1998. Bedrock fluvial incision in the tectonically active setting evaluated in the context of the stream power law and the valley-width/channel-width ratio. Abstracts with Programs-Geological Society of America Annual Meeting 30 (7), P329.

Prentice, C.S., et al., 1999. Northern San Andreas fault near Shelter Cove, California. Geological Society of America Bulletin 111 (4), 512–523.

Rantz, S.E., 1968. Average Annual Precipitation and Runoff in North Coastal California. Hydrologic Atlas, vol. HA-298. US Geological Survey, Washington, DC.

Richards, K., 1982. Rivers, Form and Process in Alluvial Channels. Methuen and Co., New York. 361 pp.

Rock, N.M.S., 1988. Numerical Geology. Lecture Notes in Earth Sciences, vol. 18. Springer-Verlag, New York. 427 pp.

Roe, G.H., Montgomery, D.R., Hallet, B., 2002. Effects of orographic precipitation variations on steady-state river profiles and relief. Geology 30 (2), 143–146.

Schumm, S.A., Dumont, J.F., Holbrook, J.M., 2000. Active Tectonics and Alluvial Rivers. Cambridge Univ. Press, Cambridge. 276 pp.

Selby, M.J., 1993. Hillslope Materials and Processes. Oxford Univ. Press, Oxford, UK. 451 pp.

Sklar, L., Dietrich, W.E., 1998. River longitudinal profiles and bedrock incision models: stream power and the influence of sediment supply. In: Tinkler, K.J., Wohl, E.E. (Eds.), Rivers Over Rock: Fluvial Processes in Bedrock Channels. Geophysical Monograph, vol. 107. American Geophysical Union, Washington, DC, pp. 237–260.

Sklar, L., Dietrich, W.E., 1999. Relating rates of fluvial bedrock erosion to rock strength: an experimental study (abstract) . EOS, Transactions-American Geophysical Union 80 (46), F448.

Sklar, L.S., Dietrich, W.E., 2001. Sediment and rock strength controls on river incision into bedrock. Geology 29 (12), 1087–1090.

Snyder, N.P., Whipple, K.X., Tucker, G.E., Merritts, D.J., 1999. Evidence for an equilibrium between main-trunk-channel incision and tectonic uplift: Mendocino triple junction region, northern California. Annual Meeting Expanded Abstracts, Geological Society of America 31 (7), 444–445.

Snyder, N.P., Whipple, K.X., Tucker, G.E., Merritts, D.J., 2000. Landscape response to tectonic forcing: DEM analysis of stream profiles in the Mendocino triple junction region, northern California. Geological Society of America Bulletin 112 (8), 1250–1263.

Snyder, N.P., Whipple, K.X., Tucker, G.E., Merritts, D.J., 2003. The importance of a stochastic distribution of floods and erosion thresholds in the bedrock river incision problem. Journal of Geophysical Research (in press).

Stock, J.D., Dietrich, W.E., 1998. Channel incision by debris flows: a missing erosion law? EOS, Transactions-American Geophysical Union 79 (45), F366.

Stock, J.D., Dietrich, W.E., 2003. Valley incision by debris flows: evidence of a topographic signature. Water Resources Research (in press).

Stock, J.D., Montgomery, D.R., 1999. Geologic constraints on bedrock river incision using the stream power law. Journal of Geophysical Research 104, 4983–4993.

Strand, R.G., 1962. Geologic Map of California, Redding Sheet. Department of Conservation, State of California, Sacramento, CA.

Talling, P.J., 2000. Self-organization of river networks to threshold states. Water Resources Research 36 (4), 1119–1128.

Tinkler, K.J., Wohl, E.E., 1998. A primer on bedrock channels. In: Tinkler, K.J., Wohl, E.E. (Eds.), Rivers Over Rock: Fluvial Processes in Bedrock Channels. Geophysical Monograph, vol. 107. American Geophysical Union, Washington, DC, pp. 1–18.

Tucker, G.E., Bras, R.L., 2000. A stochastic approach to modeling the role of rainfall variability in drainage basin evolution. Water Resources Research 36 (7), 1953–1964.

Tucker, G.E., Slingerland, R., 1997. Drainage basin responses to climate change. Water Resources Research 33 (8), 2031–2047.

Wannanen, A.O., Harris, D.D., Williams, R.C., 1971. Floods of December 1964 and January 1965 in the Far Western States. U.S. Geological Survey Water-Supply Paper, vol. 1866-A. US Government Printing Office, Washington, DC. 265 pp.

Whipple, K.X., Tucker, G.E., 1999. Dynamics of the stream-power river incision model: implications for the height limits of moun-

tain ranges, landscape response timescales, and research needs. Journal of Geophysical Research 104 (B8), 17661–17674.

Whipple, K.X., Tucker, G.E., 2002. Implications of sediment-flux-dependent river incision models for landscape evolution. Journal of Geophysical Research 107 (B2), 10.1029/2000JB000044.

Whipple, K.X., Anderson, R.S., Hancock, G.S., 2000a. River incision into bedrock: mechanics and relative efficacy of plucking, abrasion, and cavitation. Geological Society of America Bulletin 112 (3), 490–503.

Whipple, K.X., Snyder, N.P., Dollenmayer, K., 2000b. Rates and processes of bedrock incision by the Upper Ukak River since the 1912 Novarupta ash flow in the Valley of Ten Thousand Smokes, Alaska. Geology 28 (9), 835–838.

Wohl, E.E., 1998. Bedrock channel morphology in relation to erosional processes. In: Tinkler, K.J., Wohl, E.E. (Eds.), Rivers Over Rock: Fluvial Processes in Bedrock Channels. Geophysical Monograph, vol. 107. American Geophysical Union, Washington, DC, pp. 133–151.